ANALYSIS OF THE STATIC MECHANICAL PROPERTIES OF ZINC OXIDE NANOPARTICLE COATED SILK WASTE REINFORCED POLYESTER BIO-COMPOSITE.

By:

TUMUSIIME GODIAS

TEC/PGMT/08/18

A Thesis Submitted in partial Fulfillment of the Requirements for the Award of the Degree of Master of Science degree in Textile Engineering, Department of Manufacturing, Industrial and Textile Engineering, Moi University-Eldoret, Kenya

June, 2022

DECLARATION

DECLARATION BY THE STUDENT

This thesis is my original work and has not been presented for a degree in any other university or educational institution. No part of this thesis may be reproduced without prior written permission by the author and/or Moi University.

Signature:  _____ 6th June 2022

Tumusiime Godias Date

TEC/PGMT/08/18

DECLARATION BY SUPERVISORS:

We declare that this thesis has been submitted for examination with our approval as university supervisors.

Signature:  _____ 4th June 2022

Prof. (Eng.) P. M. Wambua, FIEK Date

Moi University, Eldoret, Kenya

Signature: 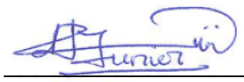 _____ 6th June 2022

Dr. S. Rwahwire Date

Busitema University, Tororo, Uganda

DEDICATION

I dedicate this thesis to my loving mother Mrs. Kemiziga Beatrice, my lovely wife Natukunda Beth and my daughters Bernice Atukunda Tumusiime and Belicia Aturinda Tumusiime. Thank you for your love, encouragement, support and the sacrifices you made to ensure I succeed.

ABSTRACT

There has been an increasing trend of using natural fibre reinforcements as an alternative to manmade fibre reinforcements for engineered composite applications. Natural fibres are alternative composite reinforcement materials due to their biodegradability, inexpensiveness, abundance and excellent physical properties. This study aimed at analysing the mechanical properties of the fabricated bio-composite from polyester resin reinforced with silk waste fabric. The specific objectives of this work were to characterise physical and mechanical properties of silk waste fabric, fabricate a bio-composite from silk waste fabric treated with zinc oxide nanoparticles and polyester resin and to analyse the static mechanical properties (tensile, flexural, and impact). The silk waste fabric was characterized and the composite fabricated using hand lay-up technique and a mould with dimensions 360x210x4 mm. Central Composite Design was used in the design of experiments and the fibre weight fraction was varied from 11 to 25%. Treatment with nanoparticles was done by soaking silk waste fabric in a 6% concentration of Zinc oxide nanoparticles and 1% citric acid. A sonicator was used to evenly distribute the nanoparticles in the solvent and the fabric was coated using the pad dry cure method. The fabricated composites were cured at room temperature for 24 hours under consolidated pressure of 2.65 kN/m^2. The mechanical properties of the composites were determined using D790, D638 and D6110 ASTM standards whereas the morphology was investigated using a Scanning Electron Microscope (SEM) and Fourier Transform Infrared (FTIR) and the thermal properties evaluated by Thermal Gravimetric Analysis (TGA). The areal density of the silk waste fabric was 76 g/m^2 and its tensile strength was 16.80 MPa. The tensile, flexural and impact strengths of uncoated composites were 27.92 MPa, 52.13 MPa and 32.17 kJ/m^2 respectively. The flexural and tensile strengths of the coated bio-composites increased with increasing fibre weight fraction up to peak values of 32.23 MPa and 53.47 MPa respectively. Bio-composites produced with silk waste fabric treated with nanoparticles had slightly better strengths (tensile 32.23 MPa and flexural 53.47 MPa) compared to bio-composites with non-treated silk waste fabric (tensile 27.92 MPa and flexural 52.13 MPa). The static mechanical properties attained in this study revealed that these bio-composites may be used for non-structural applications for instance partitioning walls and ceiling boards. The study recommended future research works on coating of silk waste fabric with nanoparticles using thermal evaporation technique and analysis of the effect of increasing the number of plies with stacking sequence of angles on mechanical and thermal properties of the composites and morphology.

TABLE OF CONTENTS

LIST OF TABLES

LIST OF FIGURES

ACKNOWLEDGEMENTS

My heartfelt gratitude goes to the Lord God almighty for guiding me through this journey and granting me sufficient grace and wisdom every step of the way.

I would like to thank the African Centre of Excellence in Phytochemicals, Textile and Renewable Energy (ACEII-PTRE), Moi University, for the scholarship which enabled me to study towards this Master's degree. A special thank you goes to the project centre leader, coordinator, secretary, the administrators and the accountant for ensuring the smooth operation of this scholarship. I would like also to thank the African Centre of Excellence in Materials, Product development and Nanotechnology (ACEII-MAPRONANO) Makerere University Kampala Uganda for the research support fund rendered to me for the completion of this research work. My utmost gratitude goes to my supervisors Prof. (Eng.) Paul. M. Wambua, FIEK and Prof. Samson Rwahwire for their tireless support, patience, guidance and advice throughout this research. I would also like to thank my other lecturers; Dr. David Njuguna , Prof. Josephat Mwasiagi, Dr. Eric Oyondi, Prof. John Githaiga, Dr. Charles Nzila and Dr. Jerry Ochola. I am also thankful to Mr. John Khafafa for the practical assistance during my experiments.

I also take this opportunity to thank the staff of the Department of Polymer, Textile and Industrial Engineering at Busitema university especially Dr. Nibikora Iledephose for the guidance that enabled me to perform my experiments in materials and metallurgy and Textile laboratories. Many thanks to my fellow colleagues and friends with whom I interacted during the course of my studies at Moi University. I appreciate the friendship, motivation and encouragement. Thank you for making my experience a pleasant one

LIST OF ACRONYMS AND ABBREVIATIONS

ABBREVIATION	DEFINITION
ALD	Atomic Layer Deposition
ASTM	American Society for Testing and Material
BTCA	Butane Tetra Carboxylic Acid
CCD	Central Composite Design
DID	Drawing In Draft
FTIR	Fourier Transform Infra-Red
GO	Graphene Oxide
NARO	National Agricultural Research Organization
PHB	Polyhydroxybutyrate
SE	Secondary Electrons
SEM	Scanning Electron Microscope
UIRI	Uganda Industrial Research Institute
UPR	Unsaturated Polyester Resin
ZnO NPs	Zinc Oxide Nanoparticles

CHAPTER 1: INTRODUCTION

1.1 BACKGROUND OF THE STUDY

Silk fiber is a natural biodegradable protein filament fiber. It is highly crystalline with an organized structure. The bombyx mori is unruffled of 5507 amino acids that contain dual essential fibroin strands covered by gum-like sericin proteins. Silk fibre possess a number of properties such as compressibility, extensibility and great strength**.** With such properties the composites made from silk can be used instead of using manmade fibres (Govindaraju & Jagannathan, 2018a; Hai-yan Wang et al., 2015), though the bombyx mori uncooked silk fibres turned from silkworm cocoons remain comparatively high cost. The mulberry silk (Bombyx mori) is widely used silk for commercial applications. Sericin takes about 22.5% of mulberry silk and it is always washed off. The fibroin consists of 75% which is used as fiber in many applications (Khan et al., 2015). Silk is an endless strand of protein fibre due to the uniqueness of the features of length, fineness, luxury appeal and strength, and is always referred to as the "queen of fabrics"(Mondal et al., 2016).

However, silk waste fibres instigated after bombyx mori can be technically offered at little price. During subsequent processing of silk fibres, more silk waste can be obtained in abundance especially at reeling process (Darshan et al., 2016)**.** Silk waste is an important by-product of silk industry, mostly in developing countries which gives approximately 10% of silk waste especially on both machine and hand reeling processes of silk (Ruoyuan et al., 2009).

A composite material can be defined as a physical combination of two or more materials that results in better properties than when the individual components are used alone (Aisyah et

al., 2021; Hoang, 2015; Ibrahim et al., 2016). The main characterization of composite materials include mechanical properties such as tensile and flexural strength (Murugan et al., 2014). Natural fibers, when compared to synthetic fibers, have some shortcomings, for example, comparatively inferior mechanical properties and reduced compatibility with polymer mediums particularly thermoplastics. These short comings limit the application of natural fibers in composite production. Recent research has shown that nano-particles coated on synthetic fibers enhances their mechanical and interfacial adhesive properties (Hongguang Wang et al., 2015). Considering different surface modification techniques which have been used in treating natural fibres for composite manufacture, there is still a challenge of poor adhesion interaction between the matrix and reinforcements. Therefore, this study aims at treating the surface of natural fibers with nanoparticles to increase surface adhesion with polyester resin, hence, increasing mechanical properties.

1.2 STATEMENT OF THE PROBLEM

In recent times, there has been growing concerns about environmental pollution caused by continued use of petroleum-based materials that are completely non-degradable. In addition, these materials contribute to climate change through greenhouse gas emissions during manufacture and incineration.

In order to mitigate the negative effects of the use of these non-biodegradable materials, natural fibres may be used as reinforcements in polymer composites.

Silk is a natural fibre with good mechanical properties and thus a good candidate for use as a reinforcement in polymer composites. Furthermore, in order to propagate the ideals of circularity, silk waste may also be used as reinforcement.

During the silk reeling process, over 35% of the cocoons are left as wastes. In this study silk wastes will be utilized as reinforcement in the polymer bio-composite.

1.3 JUSTIFICATION OF THE STUDY

Darshan et.al, (2016) established the global annual production of silk fibres was 150,000 tons in 2016. Therefore, the expected silk waste was 15000tons. The wastes are obtained on machine and hand reeling processes and are normally disposed of. The utilisation of silk waste as reinforcement in a composite of suitable mechanical and thermal properties will not only enhance value but also the green effect. The current research contributes in meeting the Uganda Vision 2040 no.293 which is to attain a green and clean environment with no water and air pollution and Kenya Vision 2030 no.4 which is to live in a clean, secure and sustainable environment (Www.planning.go.ke, 2012). The research work is expected to contribute in the creation of employment opportunities through establishment of small and medium enterprises (SMEs) specialising in the manufacture of bio-composites.

1.4 OBJECTIVES OF THE STUDY

1.4.1 Main objective

The general objective of the study was to study the static mechanical properties of bio-composites made from polyester resin and Zinc oxide nanoparticle coated silk fabric.

1.4.2 Specific objectives

The specific objectives of the study were to:

i. characterize physical and mechanical properties of silk waste fabric

ii. fabricate bio-composites of polyester resin reinforced with ZnO nanoparticle coated silk fabric

iii. characterize static mechanical properties (tensile, flexural and impact) of the bio-composite

1.5 SCOPE OF THE STUDY

This study was limited to the fabrication of uncoated and Zinc oxide nanoparticle coated silk waste fabric reinforced polyester bio-composites using hand layup technique and determination of their tensile, flexural and impact static mechanical properties. The fabric was plain woven on a handloom at Uganda Industrial Research Institute using waste yarns collected from a weaving machine. The scope of the study also included characterisation of the bio-composite using FTIR, SEM and TGA.

1.6 SIGNIFICANCE OF THE STUDY

The use of silk waste as reinforcement in polymer composites is expected to minimize the challenges associated with petroleum-based synthetic fibres such as health risks and high energy consumption. In addition, biodegradable reinforcements will make a positive impact on the environment as well as reduce reliance on petroleum-based fibres in the manufacture of composites. Furthermore, application of nanoparticles is expected to help solve the current limitation of the use of environmentally friendly composites in engineering applications due to their inherent low mechanical properties.

1.7 RESEARCH QUESTIONS

1. How can silk waste fabric be easily modified before making a composite

2. Which methods is suitable for coating zinc oxide nanoparticles onto silk waste fabric
3. Can the mechanical properties of composites be improved after coating silk waste fabric with zinc oxide nanoparticles

CHAPTER 2: LITERATURE REVIEW

2.1 SILK FIBRES

Silk is one of the strongest known natural fiber with outstanding mechanical properties under both tension and compression loading (Cheung et al., 2009; Govindaraju & Jagannathan, 2018a). The potential of silk is of great importance because of its properties and structure. Silk contains greatly organized proteins and shows wide-ranging properties such as great elongation, extraordinary tensile strength and resilient to chemical attack (Ramamoorthy et al., 2015; Saravana & Mohan, 2013). The Bombyx mori is the best silk in terms of quality and is the most commonly used in textile and industrial applications. Figure 2. 1 shows a raw cocoon silk of a bombyx mori.

Figure 2. 1: Raw cocoon silk of a bombyx mori.

Silk cocoons are cooked softly in a mild soapy solution which makes sericin to dissolve and reel the silk fibers under a process known as degumming. Degumming treatment is generally done by soaking the silk fiber in boiling water (Ramamoorthy et al., 2015), among other methods. Sericin can also be removed by other degumming approaches like alkali, acid, foam, synthetic cleaner, great pressure, heat and enzyme (Ninpetch et al., 2015).

Silk fibres have advantages over synthetic fibres such as recyclability, renewability, and biodegradability and non-toxic properties as indicated in table 2.1 below. However, bombyx

mori silk fibres have high cost but silk waste fibres derived from bombyx mori can be industrially available at extremely low cost. This is because silk wastes are in abundance at the reeling process (Darshan et al., 2016).

Table 2.1: Comparison of production and environmental properties of silk and glass fibres

Features	Silk	Glass
Chemical nature	Proteinaceous	Silica based
Annual global production of fibres (tons)	150,000	4,000,000
Biodegradable	Yes	No
Recyclable	Yes	Partly
Renewable source	Yes	No

Table 2.2 indicates different properties of mulberry silk fibres

Table 2.2: Properties of mulberry silk

Fiber	Extensibility (%)	Degree of crystallinity (%)	Thermal degradation (^{0}C)	Maximum temperature(^{0}C)	Tensile Strength (GPa)
Mulberry silk	18-47	38-66	250	170	0.6

2.1.1 Silk processing

Mulberry cultivation is the essential operation in silkworm rearing. The silkworms feed on mulberry leaves. The mulberry leaves are cut to supply the silkworms as their feeds. Rearing of silkworms are majorly larvae of the silk moth and they spin into cocoons at that stage through a spinneret at their heads. Larvae are placed in special trays and then to rooms with controlled temperature and humidity. This follows regular feeding with mulberry leaves. The reeling process involves the removal of silk filaments from the cocoons by cooking them in

water. This makes it to remove sticky gum (sericin) in the silk, which aids silk binding and unwinding into filament yarns. Mostly 8-10 cocoons are combined together to make one filament yarn (P. Bhatt, 2011; Li & Hu, 2006) There are a number of silkworm species such as mulberry silk (Bombyx mori) which consist about 95% of world's silk production estimates. Others silk species are eri silkworm, indian tasar and muga silkworms (Li & Hu, 2006).

The tensile strength of silk ranges between 125–420 MPa and its elastic modulus 8.9–17.4 GPa. Silk has a density of about 1.3 g/cm and is a rather uniform continuous fibre (Fuqua et al., 2012).

2.1.2 Silk waste.

Silk is not only a high-class fibre but also offers other important valuable wastes and by-products like recycled silk yarns, pupae, sericin and pupae oil as shown in Figure 2.2. Twisted silk yarns find use in different textile applications (Javali et al., 2015).

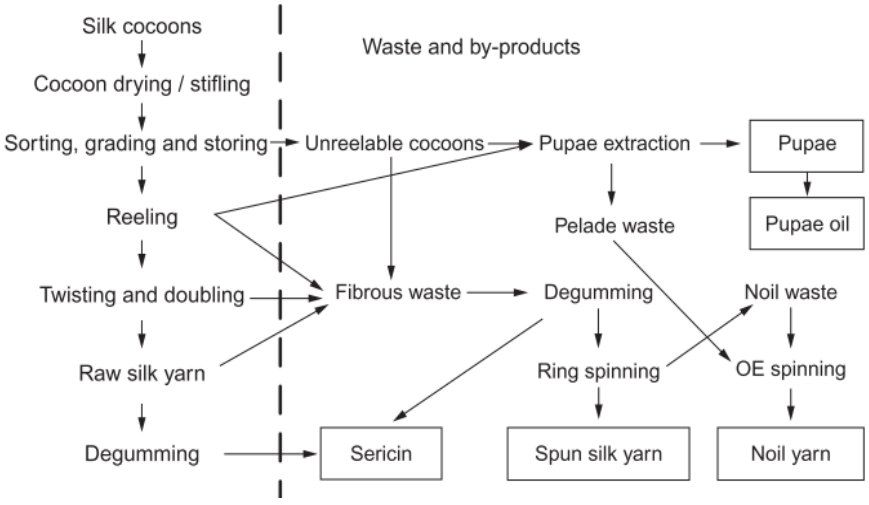

Figure 2.2: Brands of discarded and by-products of silk manufacturing.

Approximately 35% of the raw silk remains and imperfect cocoons are processed into a strand named silk straw. A manual method of cooking is utilized to soften the sericin of the cocoons. The yarns are then used to make interlaced fabrics. The yarns have a great quantity of sericin which makes their treating hard, consequently it desired that it should be s to be removed by conservative degumming routes. Subsequently, degummed silk straw filaments can be converted into cloths using the intertwining route (Arakem et al., 2017).

2.1.2.1 Silk waste composites

The success of natural fiber reinforced polymeric composites is majorly dependent upon appropriate manufacturing techniques and surface modification of fibers to improve the adhesion between matrix and the reinforcement so as to improve performance as well as long-term durability and fire retardancy (Faruk et al., 2013). Cheung et al.(2008) studied silk fibres and their findings confirmed that silk can be used as a reinforcement in composite manufacture. The treatment of silk/polyester composites with alkali solution was studied by Noorunnisa et al. (2007). Their findings showed the tensile and flexural strengths of the treated composites increased by 24.4% and 17.7% respectively. This indicated that the treatment of silk fibres enhanced the mechanical properties (Noorunnisa et al., 2010). Kim et al., (2006) studied polybutylene adipate/nanotube coated on silk fibres composites and reported an increase in the mechanical properties with the incorporation of 3wt% carbon nanotube coated silk fibers.

The mechanical properties of Silk/Epoxy Composites were studied by Hamidi et. al. (2018) and the results showed an increase of 23% on the flexural properties. This was attributed to the treatment of silk fibres. Nourbakhsh et. al., (2018) studied the coating of ZnO nanoparticles onto polyester fabric through alkali treatment and their findings indicated improved chemical bonding under FTIR analysis. Tasdemir et al, (2008) studied the properties of recycled waste silk and cotton fiber

polymer composites and reported an improvement of the physical and mechanical properties of the composite structures for different applications.

2.1.3 Characterisation of fibres

In the characterization of fibres, tests are carried out to determine the behaviour and nature of the fibres. The physical and mechanical tests include tests for fibre length, fibre strength, fibre fineness and moisture regain of fibres.

2.1.3.1 Fibre strength

Tests on single fibres can be accepted out on a universal tensile tester with the appropriate load cell and lightweight clamps. The ASTM D3822 for single fibre strength test stipulates gauge length of 12.7 mm or 25.4 mm and up to 40 fibres should be tested. The gauge length of 10, 20 or 50mm with a testing speed of 0.1mm/min such that the sample fibre ruptures in 20-30 seconds were used. The least number of tests is 50 and pretension is 0.5gf/tex. In bundle fibre strength testing a bunch of fibres are put into two jaws of a universal tensile tester. The jaws are moved until the fibres break. The fibre tenacity (strength) is calculated as shown in equation 2.1.

$$Tenacity\ of\ the\ fibre\ \frac{G}{Tex} = \frac{Breaking\ load\ kg * length\ of\ sample\ in\ mm}{mass\ of\ the\ fibres\ in\ mg} \qquad \text{Equation 2.1}$$

It is advisable to use the same gauge length for all tests, selecting it to accommodate the shortest fibre of interest (Indran & Raj, 2015)

2.2 POLYESTER RESIN

Polyesters can be classified into two groups: saturated and unsaturated. The saturated polyesters are thermoplastic while the unsaturated ones are thermosets. The most common polyesters are thermoplastics based on PBT (Polybutylene terephthalate) and PET (Polyethylene terephthalate). Polyester resins, on the other hand, are cured by hardeners and are commonly used in the manufactures of composites.

Polyester is commonly used for a number of applications. These include labelling, packaging, textiles, laboratory equipment, polymer banknotes, stationery and plastic parts.

2.2.1 Properties of unsaturated Polyester resin

. The properties of unsaturated polyester resin are presented in Table 2.3. The resin can be used as a matrix in composite materials (Ogunsile & Oladeji, 2016).

Table 2. 3 Properties of Polyester resin

Property	**Range**	**Property**	**Range**
Tensile Modulus (GPa)	0.8-1.2	Shrinkage (%)	0.005-0.009
Tensile strength (MPa)	15-20	Density(g/cm^3)	1-1.3
Flexural modulus (GPa)	1.1-1.6	Young's modulus (GPa)	4-6
Compressive strength (MPa)	80-220	Specific gravity	1-1.5
Flexural strength (MPa)	25-32	Poisson ratio	0.45

2.3 NANOTECHNOLOGY

Nanotechnology is defined as the production, design and usage of nanostructured structures. Nanoparticles have constituent part dimension of 1 to100 nm and have a superior surface area per weight compared to bigger elements (Selvaraj et al., 2014). Nanotechnology can be applied to enhance performance of bio-composites by providing nanotechnology-based

coats to decrease water uptake and biodegradation and increase flame resistance (Faruk et al., 2013). (Faruk et al., 2013).

Nadiger & Shukla, (2016) worked on the application of butane tetra carboxylic acid on silk in the presence of sodium hypophosphite concurrently with silver nanoparticles prepared by pad-dry-cure method. Application of 6% BTCA with 3% SHP and 250 ppm of silver nanoparticles provided satisfactory antimicrobial properties. The FTIR studies showed good cross-linking of BTCA and the X-ray diffraction results indicated the crystal arrangement and crystallinity percentage of preserved silk did not alter due to the treatment

2.3.1 Methods of coating nanoparticles onto fabrics

2.3.1.1 Atomic layer deposition (ALD)

The ALD procedure involves a hot-wall fastened chamber-type reactor employing nitrogen as a precursor carrier and purge gas. In this process, silk fabric was placed in the ALD reactor and allowed to dry at 100 ºC for 10 minutes in a vacuum of 20 Pa using a stable nitrogen gas stream of 20 standard cubic centimeter (SCCM). TiO_2 admission was achieved by combining appropriate doses of titanium tetraisopropoxide (TTIP) and H_2O. To yield satisfactory vapor pressures, the TTIP temperature was maintained at 60ºC, while the H_2O was kept at room temperature. The carriage line from the predecessor vessel to the apparatus chamber was sustained at 100 ºC, and the typical deposition temperature castoff in this study was 100 ºC. The graphic procedure of TiO_2 ALD on silk fibers is displayed in Figure 2.3. The simple ALD procedure cycle is concisely styled into two half reactions (Xiao et al., 2015).

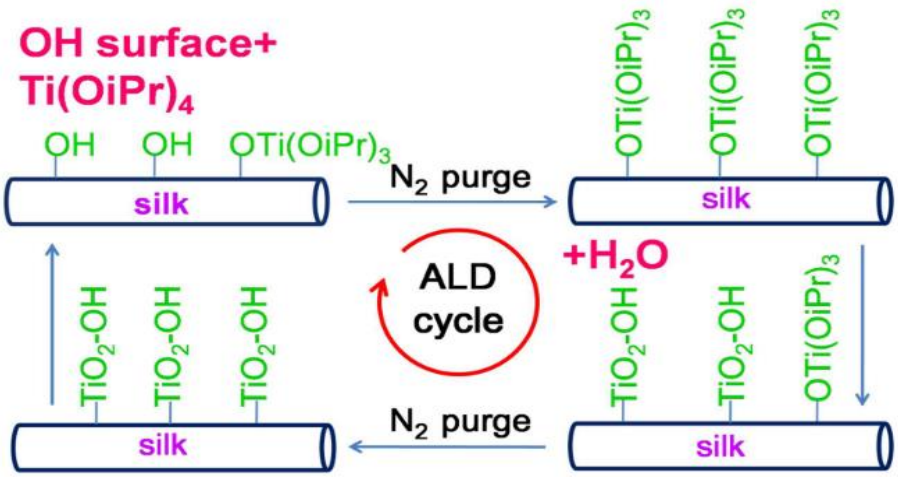

Figure 2. 3 The graphic route of TiO2 ALD on silk fibers.

2.3.1.2 Layer-by-layer deposition method

The covering of silk fibers with ZnO nanoparticles was carried out using the layer-by-layer deposition process. In this technique, electrostatic interfaces between oppositely charged polyelectrolytes can be cast-off with anionic silk surface and cationic zinc ions (Khanjani et al., 2013; Rani et al., 2019).

2.3.1.3 Thermal evaporation system

ZnO nanoparticles can also be layered on silk fabric by means of thermal evaporation system. This is a dry clean method because it eludes waste and reduces the usage of target powder. The use of ZnO NPs on textile fabrics is intended to yield antibacterial fabrics. There are a number of methods used for coating for instance melt, dip, drop and chemical vapour deposition (Ghiasi et al., 2014). Figure 2.4 indicates the representation of nanoparticles

synthesis with (a) indicating the emulsification and (b) two step desolvation methods respectively (Sundar et al., 2010).

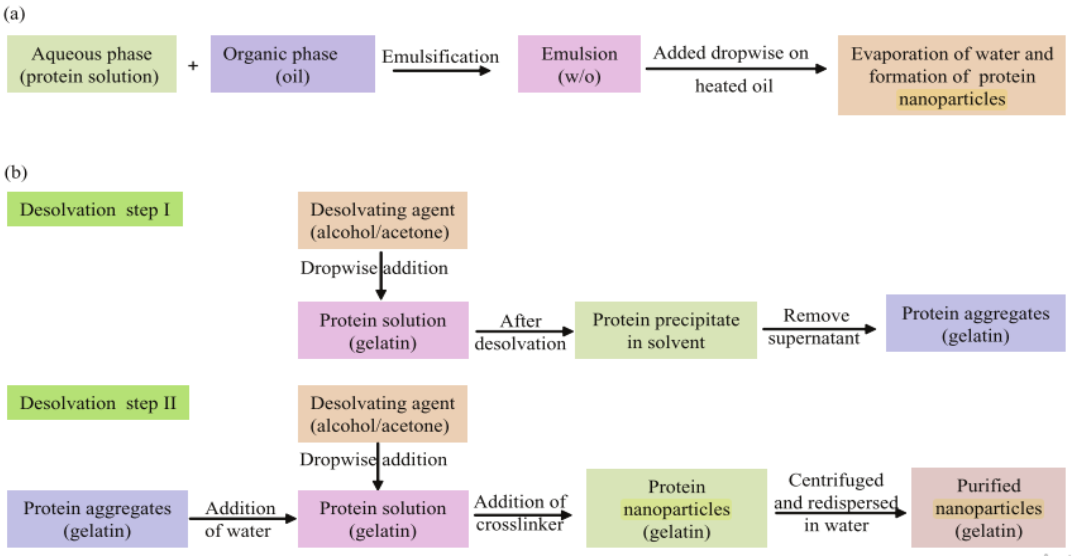

Figure 2.4: Schematic representation of nanoparticles preparation.

2.3.1.4 Pad dry cure method

The introduction of new functional groups to fiber surface using TiO_2 nanoparticles to solve the problem of stability and durability was done by a pad dry cure method. In addition, TiO_2 thin film was produced on cotton fabric from a colloidal sol by a simple dip pad dry cure process in a short time. TiO_2 film/cotton adhesion was enhanced with good fastness (Gashti et al., 2012; Zhang et al., 2014). Conventional pad-dry- cure process can be easily used to apply an emulsion of chitosan-silver oxide nanoparticles onto textile fabrics (Allam, 2011) and is commonly used in other textile nanocoatings (Parvinzadeh Gashti et al., 2016).

2.4 CHARACTERIZATION OF NANOPARTICLE COMPOSITES

Material characterisation is the study of materials' structures for example its composition, structures and properties. This can be done by using innovative equipments such as scanning electron microscopy and transmission electron microscopy. Properties like the average particle diameter, dimension distribution, and charge affect the physical stability and the in vivo distribution of the nanoparticles. Properties such as size, surface morphology and overall shape are determined by electron microscopy techniques. The surface charge of the nanoparticles is altered by features like physical stability. During the characterization of nanoparticle, it is very vital to estimate the surface charge (Bhatia, 2016). This is achieved by using both scanning electron microscopy (SEM) and transmission electron microscopy (TEM) because of the high resolution and high imaging speed, with the standard methods for direct imaging and dimensional measurements of micro- and nanostructures (Buhr et al., 2009).

2.4.1 Scanning Electron Microscopy (SEM)

This scanning electron microscopy-based method defines the shape, surface morphology and size with direct imagining of the nanoparticles. Therefore, SEM offers several advantages in morphological and sizing analysis. The use of SEM, however provides inadequate information about the scope distribution and true population average during operation. The nanoparticle which is in solution should be changed into a dry powder. The powder is then placed on a sample holder by coating it with gold using a sputter coater. The sample is analyzed by scanning with a focused fine beam of electrons. The surface characteristics of the sample are characterized by secondary electrons (SE) radiated. The presence of an

electron beam often damages the polymer of the nanoparticles which must be able to withstand vacuum (Bhatia, 2016). The surface of fibers is always coated with gold prior to SEM inspection to improve on the conductivity properties of samples. The pictures are always taken at a slow scanning speed to obtain higher quality image (Jabbar, 2017).

2.4.1.1 The basic principle of SEM

In the basic principle of SEM shown in Figure 2.5, the electron beam attacks the surface of the specimen and interrelates with the atoms of the sample. The secondary electrons with their signals, back scattered electrons and X-rays are generated which contain information of the sample's features such as surface topography and composition. The scanning produces a very high-resolution images of a sample surface to a range of 1-5 nm in size in its primary detection mode (Joshi et al., 2008). The SEM lessons were directed with an electron beam accelerating potential of 3 kV (Indran & Raj, 2015).

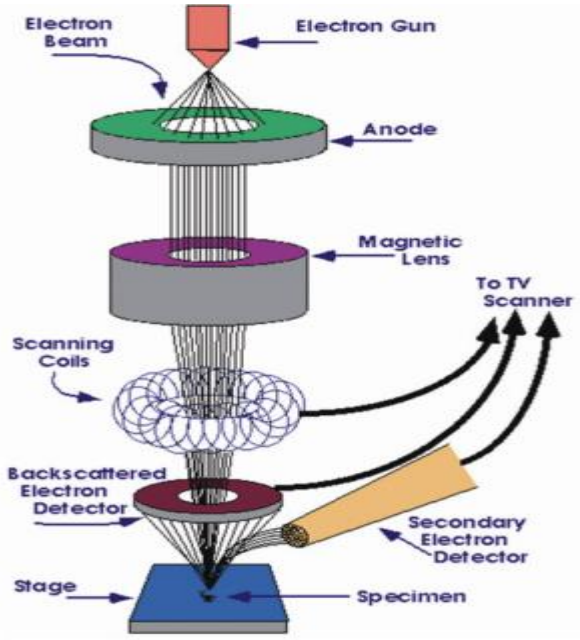

Figure 2.5: Scanning electron microscopy with its main components.

2.4.2 Fourier Transform Infra-Red (FTIR)

FTIR analysis was cast-off to originate the FTIR spectra of the root fiber in KBr matrix with a scan rate of 32 scans per minute at a determination of 2 cm^{-1} in the wave number region 400–4000 cm^{-1}. The cut samples were stranded to fine powder using a mortar and pestle and then varied with KBr. They were then pelletized by smearing pressure to make the specimen to greatest the FTIR spectra under standard conditions. FTIR spectra are cast-off to regulate the presence of free functional groups in fibre (Indran & Raj, 2015).

2.6 MANUFACTURING TECHNIQUES FOR THERMOPLASTIC COMPOSITES

2.6.1 Autoclave consolidation process

Autoclave moulding is a composite manufacturing method that uses pressures in excess of atmospheric to produce critical products. The plies or prepregs are vacuum bagged before being placed inside the autoclave (Nevres, 2009) with computer-controlled temperature and pressure This method produces composites with very low void content which is important for high performance applications.

2.6.2 Compression molding process

Compression molding is a process whereby the feed material is pressed between the two mold halves of a compression moulding machine in order to force resin and reinforcement fibers to the cavity. The two forms of feed which are used in compression moulding are Sheet Moulding Compound (SMC) and Bulk Moulding Compound (BMC). As shown in Figure

2.6, the BMC is placed in the mould and compressed under heat and pressure. The moulds are usually made of metal because considerable amount of heat is used.

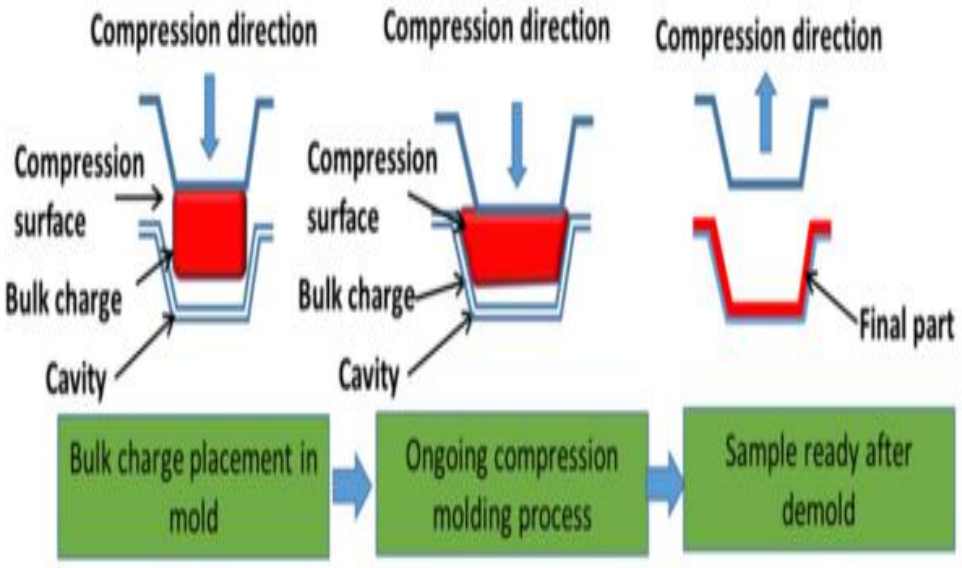

Figure 2.6: Typical compression molding method using bulk charge.

2.6.3 Hand lay-up method

This is one of the open molding processes. The reinforcement is arranged and placed on a one-sided mold. Resin is then poured onto the fabric/fiber surface and squeezed in using a hand roller. This physical rolling motion eliminates trapped air and ensures complete wet out of the reinforcement. This eventually densifies the composite. A catalyst can be added to initiate curing of the resin system. This is the simplest composites manufacturing process as shown in Figure 2.7. Hand layup is usually employed in the manufacture of low volume large structures such as wind turbine blades. The process of layering and placing the reinforcement and matrix in different directions enhances strength and stiffness of the composite (A. T. Bhatt et al., 2018).

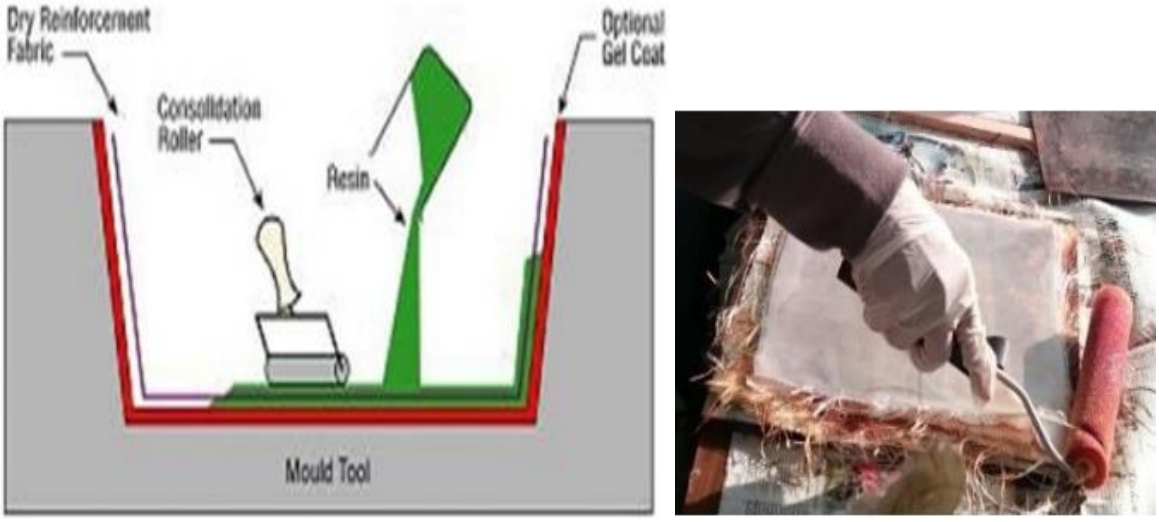

Figure 2. 7 Hand lay-up molding method.

Table 2. 4 Summary of composite manufacturing methods

Technique	**Process Details, Advantages & Limitations**	**Material/ System**	**Uses**
Hand lay-up	• In this technique, the mould is cleaned using acetone and mould release agent is applied before placing the reinforcement. • Resin is then applied with a hand brush and rollers. • The component is dried at room temperature or raised temperature **Advantages** • Method is less costly, • less time consuming • easy but can achieve low fiber volume fraction	Materials • knitted • stitched • bonded fabrics • Woven System • Thermoset such as polyester, epoxy,	• Boats, • architectural shapes • Wind-turbine blades,

Spray Layup	• The use of a spray gun is commonly applied where fusion of cut fibres with catalyst and resin is sprayed on the mould surface • the material is squeezed with rollers to get rid of trapped air	Material • particles • cut fibers • Thermoset such as unsaturated polyester resin	• Shower tray • Bath tubes • Structural panels
Filament winding	• This method involves winding of resin impregnated filaments on a mandrel, •	Material woven • Thermoset • vinyl ester • Epoxy • phenolic • polyester	• Radomes • Rotor shafts. • pressure vessels • pipes
Resin Transfer Molding	This techniques is a closed mould method. . The reinforcement is placed in the mould and resin is injected under pressure and or vacuum.	roving, cut fiber mat, Woven material, polyester resin, vinyl ester	Automotive components submarine Aircraft parts
Vacuum Assisted Resin Transfer Moulding	• This technique has one of its tool stationary and the second one flexible. • The fabric is placed on the mould, surrounded with peel ply, release film or distributor film, vacuum bag and covered by sealant tape. • The supply of resin is by use of pipe from the tank to the fabric.	Woven fabric, roving, chopped fiber mat Thermoset resin- vinyl ester, epoxy and polyester	scale wind turbine blades' bridge sections and Bar

Pultrusion	Continuous rovings from bobbins are directed to a resin tank and passed through a heated die. The pultruded composite is cut at intervals using a cutter.	rovings, Thermoset & rarely thermoplastic	pipe, bar and rod, , Beams
Compression moulding	The major considerations in compression molding method are pressure, time and temperature.	mat, woven fabric, short fibres Thermoplastic, Thermoset	Windows for the airplane, Car doors, truck parts
Centrifugal casting	In this procedure centrifugal force is applied to produce cylindrical parts with resin and cut fibers.	Chopped fibers Thermoset resin - epoxy, polyester	Large diameter cylindrical pipes, telegraph poles, cylindrical components

2.7 CHARACTERISATION OF COMPOSITE

2.7.1 Tensile strength

The sample may be tested using universal testing machine tensile tester according to ASTM D638.

2.7.1.1 The Tensile strength test procedures;

- The specimens are cut in a rectangular form with 15 cm x 2.5 cm dimensions an axle blade.
- Then gripped between the jaws of the machine and allow to run
- The average values are recorded and the testing speed adjusted accordingly
- Once the load-extension curve reaches, the performed tests are noted

- Both the load-extension at the yield point and the load and extension at the moment of rupture are noted in the computer and the results printed on papers.
- Tensile strength of the composite sample is calculated according to equation 2.2;

$$Tensile\ strength = \frac{Force(N)}{Area(mm^2)} \quad \text{Equation 2.2}$$

- Then the loads values are converted to Newtons from kgf and divided by the surface area of the specimens being tested (Indran & Raj, 2015).

2.7.2 Flexural strength test

The composite flexural strength may be determined using a universal tensile tester in accordance to ASTM D790 standard. A sample of specified dimension is cut and a load is applied in the middle of the sample under a 3-point bending fixture

2.7.2.1 Flexural strength test procedure

(i). The sample is cut to 25mm X 100mm dimensions.

(ii). The sample is mounted on a 3-point bending fixture on the flexural tester machine

(iii). The test is allowed to run until the specimen breaks and the value of the load recorded as Force.

(iv). The flexural strength is determined as shown in equation 2.3;

$$Flexural\ strength\ \delta_f = \frac{3F_{max}}{2bh^2} * L \quad \text{Equation 2.3}$$

Where;

F_{max}-Maximum load (N), L- Length between axes (mm), h- Thickness (mm), b- Width (mm),

δ_f- Flexural strength (Mpa).

2.7.3 Impact strength test

Charpy impact test of the composite is performed on an impact tester machine. A 65 x 12.7mm composite sample is prepared according to ASTM D6110 – 10. The average values of the samples are recorded then the impact strength is calculated according to equation 2.4;

$$a_{cU} = \frac{E}{h.b} * 10^3 \qquad \text{Equation 2.4}$$

Where,

a_{cU} – Charpy impact strength of un-notched specimen (KJ/m^2), h – Thickness (mm), b – Width and E is the energy absorbed (J) by breaking the test (Indran & Raj, 2015).

2.8 RESEARCH GAPS

The major research gaps from different researchers about the use of silk waste and nanoparticles in composites are highlighted in the table 2.5 below

Table 2.5: Research gaps in silk waste and nanoparticle treated materials

Authors	**Title**	**Research gaps**
(Nourbakhsh et al., 2018)	Zinc oxide nano particles coating on polyester fabric functionalized through alkali treatment	• ZnO nanoparticles treatment to compare mechanical properties with non-treated fabric
(Govindaraju & Jagannathan, 2018b)	Optimization of mechanical properties of silk fiber-reinforced polypropylene composite using Box – Behnken experimental design	• Only very few studies are available on the utilization of the silk

		waste in the development of composites
(Yang et al., 2018)	Mechanical and optical properties of silk fabric/glass fiber mat composites: an artistic application of composites	• Investigating properties of waste silk fabric-reinforced epoxy laminates and mechanical properties
(Noorunnisa et al., 2007)	Tensile, Flexural and Compressive Properties of Sisal/Silk Hybrid Composites	• Different treatment of fibres should be done enhance the understanding of the treatments.
(Shahidi et al., 2013)	Surface Modification Methods for Improving the Dyeability of Textile Fabrics	• Application of nanoparticles for surface modification of fibers
(Verbič et al., 2019)	Recent advancements on using Zinc Oxide for Useful Textile Coverings.	• Amongst the research benefits the production of diverse composites with Zinc Oxide to widen the light interest region

CHAPTER 3: EXPERIMENTAL METHODS

3.1 RESEARCH METHODOLOGY FLOW CHART

This chart as in indicated in figure 3.1 shows the steps that were followed during experimental methods. It indicates all other processes needed to accomplish the manufacture of a bio-composite from silk waste fabric /Polyester resin using hand lay-up technique.

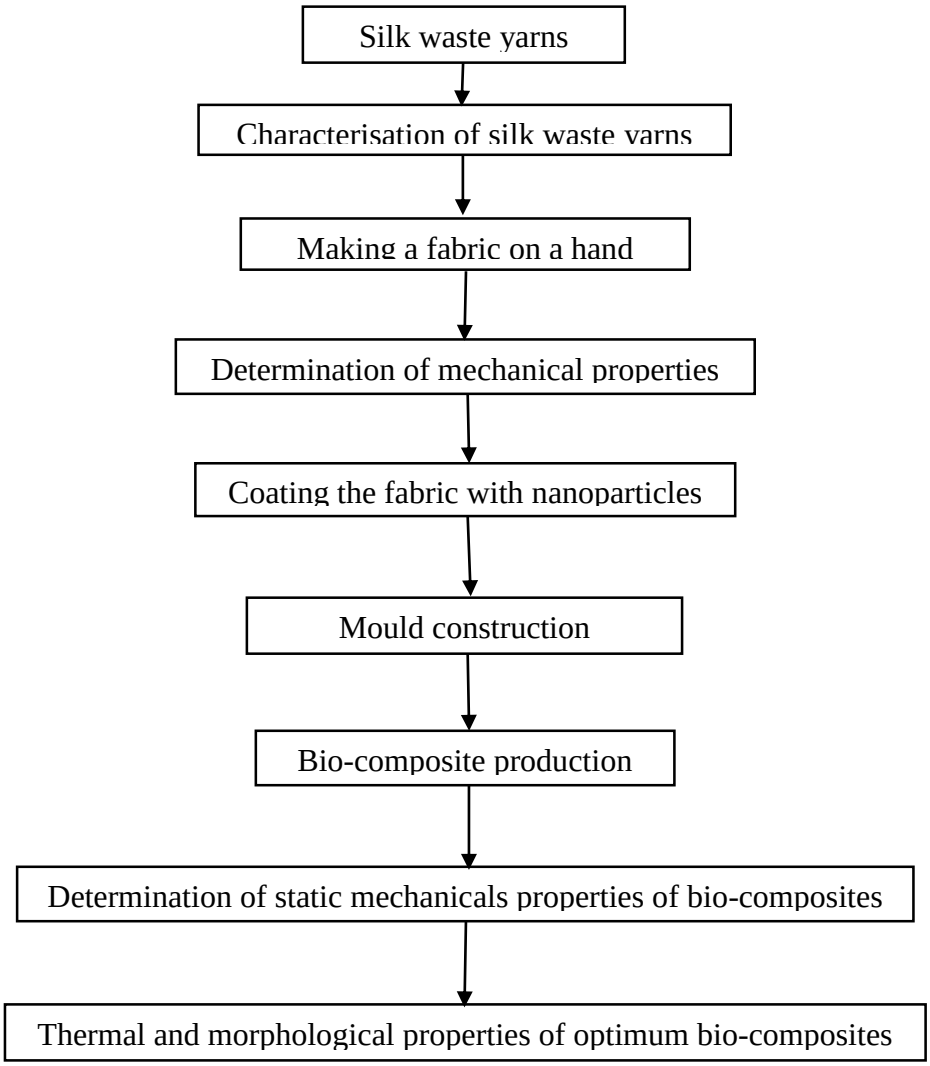

Figure 3. 1: Project methodology flow chart

3.2 MATERIALS ESTABLISHMENT

The main materials used in this research are discussed below

3.2.1 Unsaturated polyester resin, hardener and mould release

Polyester resin, hardener (methyl ethyl ketone peroxide) and mould release were sourced from Narkhi Enterprises Limited, Nairobi-Kenya. The hardener and resin were mixed thoroughly in a proportion of 1:100 by bulk as per the producer's recommendations. The matrix cures at room temperature between 10-20 minutes. The properties of UPR are as presented in Table 3.1.

Table 3. 1: Properties of the unsaturated polyester resin

Mechanical Properties	Value
Colour	Dark
Elongation at Break (%)	2.3
Density	1.232g/cm^3
Tensile Strength	29.2Mpa
Solubility	Insoluble in cold water
Flexural strength	70Mpa
Impact strength	9kJ/m^2
Elongation at break	4.2%

3.2.2 Silk waste yarns

The silk yarns waste were sourced from Uganda Industrial Research Institute (UIRI). The silk waste fabric was woven at UIRI on handloom.

3.2.3 Aluminium foil

The aluminum foil was bought from Standard Super Market near Old Taxi Park, Kampala.

3.2.4 Zinc Oxide Nanoparticles

A 100g sacket of 50nm Zinc Oxide Nanoparticles was imported from China

3.3 Determination of physical and mechanical properties of silk waste woven fabric

The tensile, flexural and impact strengths of the silk waste fabric were determined before fabrication of the bio-composite.

3.3.1 Tensile strength

The tensile strength of the silk waste fabric was determined using a Universal Testing Machine according to ASTM D638 standards. The testing was done according to the following procedures.

- The sample were cut in a rectangular form with 15 cm x 2.5 cm dimensions using a scissor.
- The woven fabric sample gripped between the jaws of the machine and allowed to run
- Different samples tested to get the average values
- Tensile strength of the woven fabric was calculated according to equation 3.1;

$$Tensile\ strength = \frac{Force(N)}{Area(mm^2)} \qquad \text{Equation 3.1}$$

3.3.2 Fabric density

The density of the silk waste woven fabric was established by weighing samples on a digital scale and determining the grams per square metre (gsm) following ASTM 6242-98 standards

3.4.2 Silk waste fabric formation

The silk waste fabric was plain woven on a handloom machine at Uganda Industrial Research Institute (UIRI) to a length of 20 metres. Figure 3.2 below shows yarns on the handloom machine at UIRI drawn through healds. Figure 3.3 below shows the fabric samples after being woven on a hand loom machine.

Figure 3.2: Silk Yarns drawn on a hand loom machine during weaving process at UIRI

Figure 3. 3: Silk fabric waste sample after being woven on a hand loom machine

3.4.3 Warps and weft per cm

The determination of the warps and wefts per cm was done using a pick glass. The weft and warp density was determined before and after degumming the fabric.

3.4.4 Determination of silk fabric waste thickness

The fabric thickness was determined using a digital thickness gauge machine (YG-141D).

3.4.5 Degumming process

Hydrogen peroxide was bought from UNILAB Kenya Limited, Nairobi. The degumming reagents were hydrogen peroxide, detergent and water. Water was boiled in the stainless sauce pan. The hydrogen peroxide and detergent were mixed together in a beaker, then the mixture was added to boiling water at 100^0c. The silk fabric was placed in the mixture, and stirring was done after an interval of 4min. The degumming process took about 20minutes. Figure 3.4 below shows the degumming process of the woven fabric using H_2O_2, detergent and water in stainless saucepan (Javali et al., 2015).

Figure 3. 4: Degumming process of woven fabric

The fabric was then removed and washed several times to remove excess chemicals. It was then dried at room temperature for a period of 24hours. Figure 3.5 shows the silk fabric samples after being degummed, washed and dried indoors.

Figure 3.5: Silk Fabric sample after being degummed and washed

3.5 Coating nanoparticles onto silk fabric

A solution of 1% citric acid was prepared in a 1 litre conical flask for nanoparticle preparation. The ZnO NPs nanoparticle colloidal suspension was coated onto silk fabric using pad dry cure method. A concentration of 6% was used in order to make a colloidal suspension easily on a sonicator machine KQ3200 (Majumder et al., 2020). Padding was done at room temperature. The coated silk fabric waste samples were then dried at 60^0c for 30 minutes and cured at 120^0c for 5 minutes in an electronic oven drier. Figure 3.6 shows the silk fabric being coated on the sonicator machine (Nadiger & Shukla, 2016).

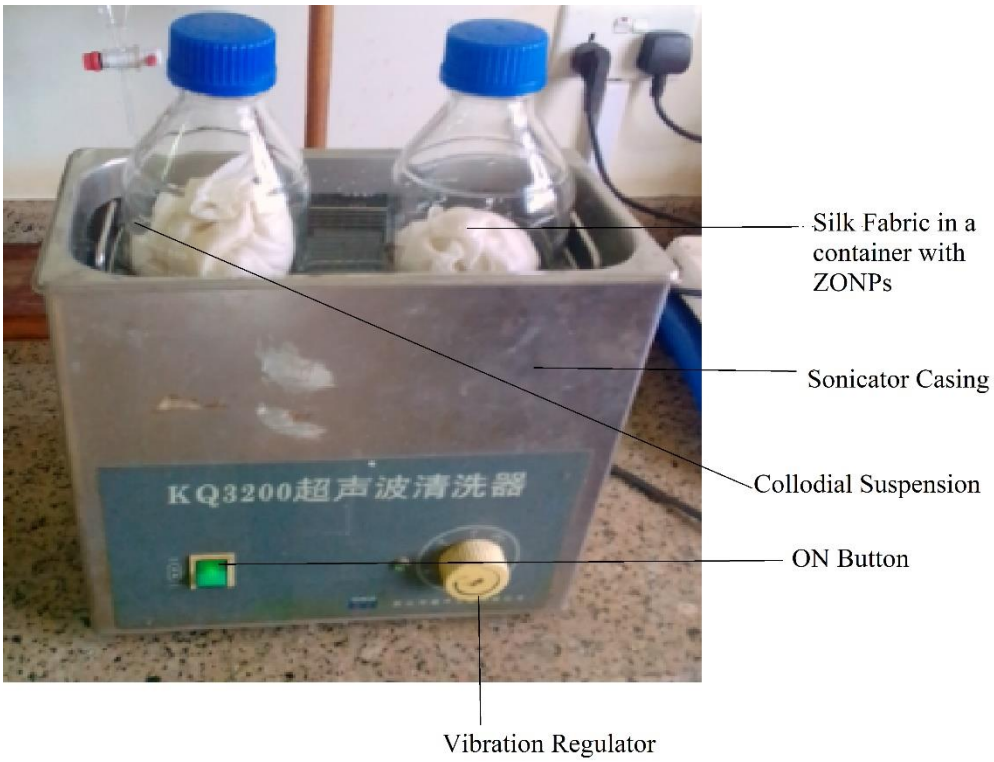

Figure 3.6 Silk fabrics being coated with ZnO NPs in KQ3200 Sonicator

3.6 Morphological, functional and thermal properties determination

3.6.1 Scanning Electron Microscope (SEM) procedures

The morphological determination of samples were carried out using a Tescan Vega 3, SBU.118-0015, Berno, Czech Republic as shown in figure 3.7. The samples were cut and fixed on a sample tab by carbon double sided adhesive carbon tape, vacuum dried and scanned at an accelerating voltage of 5kV. The adjustment knob was moved up and down until clear images were obtained and captured under secondary electron (SE) detectors.

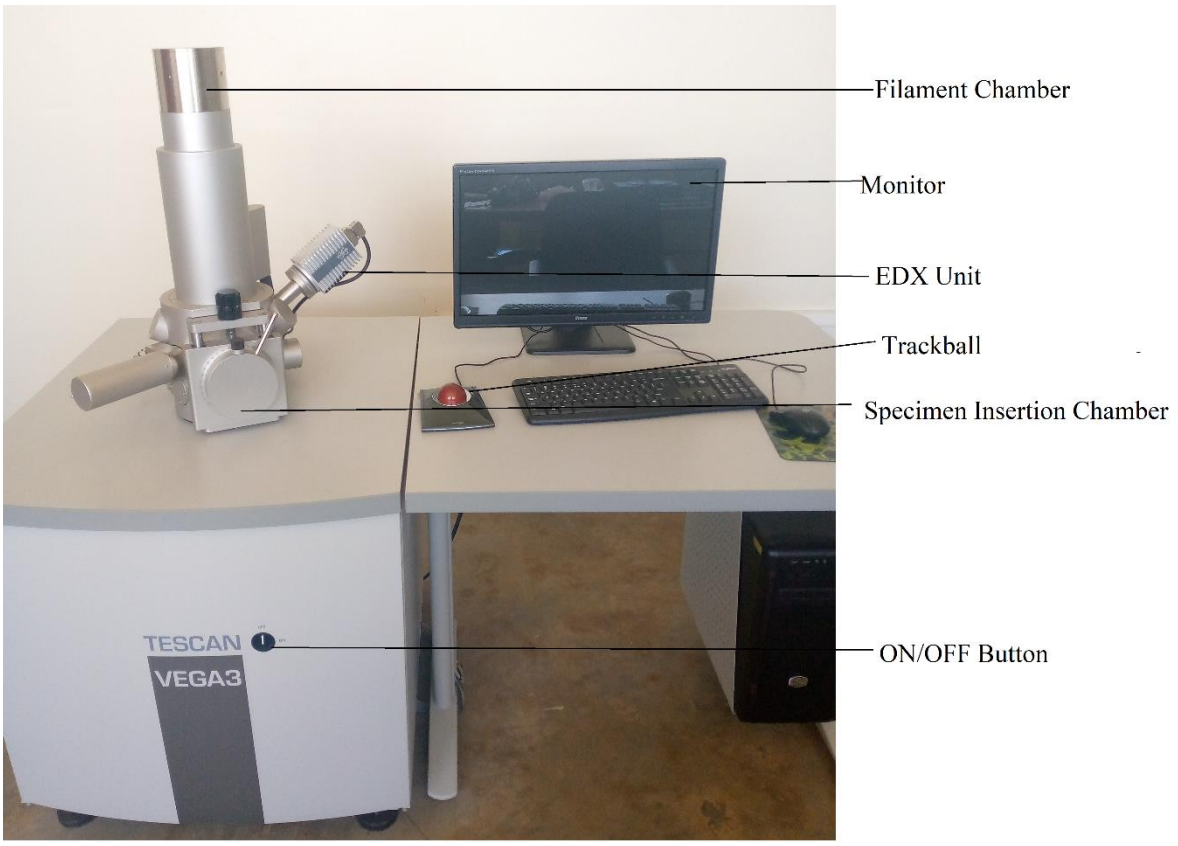

Figure 3.7 Scanning Electron Microscope in Materials Laboratory Busitema University

3.6.2 Fourier Transform Infra-Red

The functionality properties of the samples were determined using FTIR (model FT/IR-6600, Japan; M/C Serial No:-A027761790 at Busitema University in materials and metallurgy laboratory. The FTIR equipment is shown in figure 3.8 below. The FTIR analysis procedure is outlined below:

- Once the machine was on, the background was first measured without putting any sample into the machine in order to clear the existence of other particles other than the current samples being worked on.

- A graph was plotted for the background measurement.
- The machine was opened and the sample placed on the sample holder.
- The sensing lens was adjusted until it slightly touched on the sample
- Graphs of Transmittance (%) against wavenumber (cm^{-1}) were displayed and plotted.
- The scales were set for both vertical and horizontal axes from 0-100%T and 4000-400 wavenumber respectively.

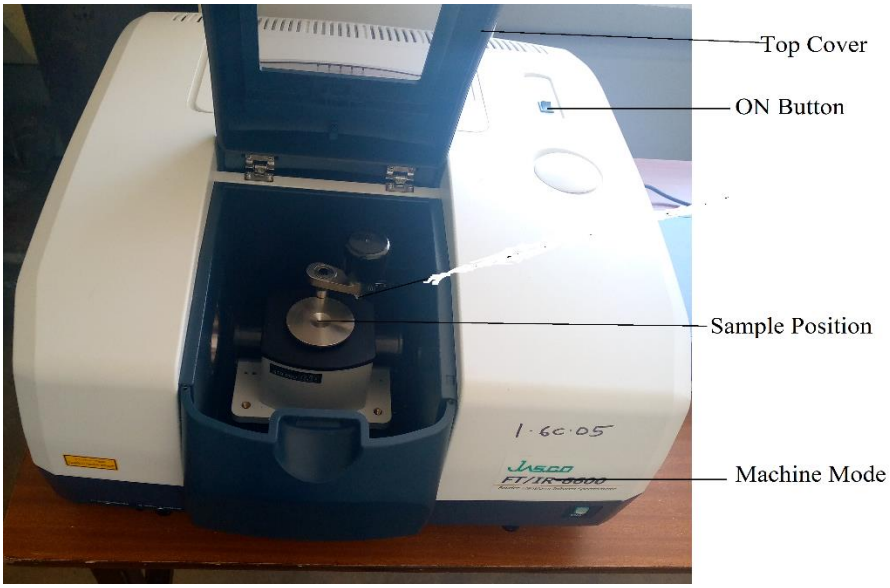

Figure 3.8 Fourier Transform Infra-Red in Materials Laboratory Busitema University

3.6.3 Thermal Gravimetric Analysis (TGA)

The thermal properties of the samples were obtained under PerkinElmer, STA 6000 simultaneous thermal analyzer, Serial no.521A17090106, Netherlands in a nitrogen atmosphere at a flow rate of 50 mL/min. The sample was weighed using precision analytical balance and the weight ranged between 10-30 mg before loading to the machine.

The actual weight of the sample was got from the machine after tare. The initial temperature was set at 30^0C and maximum to 700^0C at a rate of 10^0C/min. The change in weight with respect to temperature was programmed between the set temperatures.

3.7 Composite fabrication

A mould with dimensions 360 x 210 x 4mm was fabricated from mild steel sheet metal as indicated on Figure 3.9. The mould was cleaned with acetone and mould release agent applied. The silk waste fabric layers were cut and placed in the mould. During the fabrication of silk/polyester composites the layers of fabric were varied from 4-6 plies as proposed by Loreto et al.(2014). Silk fabric layers were laid longitudinally and the mixture of polyester and hardener was uniformly applied on the reinforcement using rollers as per the hand layup technique. The composite was allowed to cure for 24 hours (Banga et al., 2015) at room temperature under a pressure of 2.65kNm^{-2}.

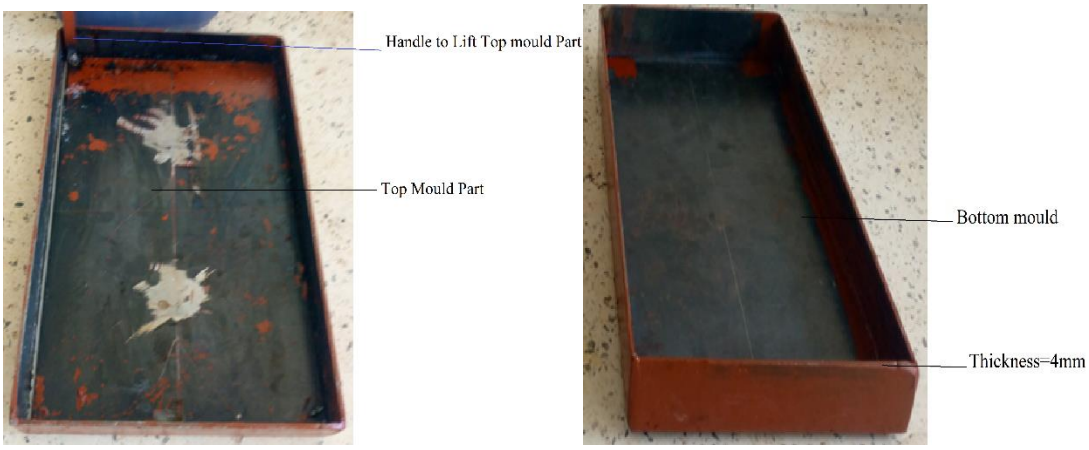

Figure 3.9: Mould dimensions for composite fabrication

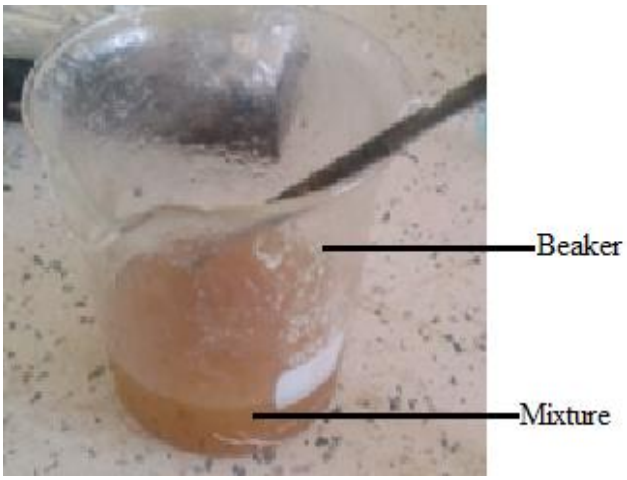

The figure 3.10 shows the mixture of resin, hardener and catalyst in a beaker.

3.7.1 Experimental design

The design of experiments was done using central composite design.

3.7.1.1 Central Composite Design

The parameters and the levels were varied according to the central composite design of experiments. The levels are represented as $-1(lower\ level)$, $-\alpha$(lower axial level), 0 (centre level), $+\alpha$ $(upper\ axial\ level)$ and 1(upper level) as shown in table 3.2 below.

Table 3. 2: Showing factors and levels in the experimental design

Factors	**Levels**				
	- α	-1	0	+1	+α
Number of plies	4	4	5	6	6
Weight fraction (%)	11	13	18.0	23.0	25

All the experimental runs were done on CCD. There were thirteen (13) experimental runs determined using equation: $N = 2^n + 2n + n_c$

Wherever; n is the number of factors n_c is the number of centre points and N is the number of runs, which ranges from 2 to 6.

Therefore, taking n_c to be 5

$$N = 2^2 + 2x2 + 5$$

$$N = 4 + 4 + 5$$

$$N = 13\ runs$$

The 13 runs were composed of five center points, four axial points and four cube points. The points of the centre in axial were considered to be zero. Star points were added to cater for quadratic relationship between response and independent variables(Azam et al., 2014).

Alpha $\alpha = 2^{k(1/4)}$ wherever K is denoted as the number of factors**.** For this case there are two factors which implies that $\alpha = 2^{2(1/4)}$ which is equal to 1.4142. The value of alpha was 1.4142 according to CCD with three levels, then, to acquire value for the axial point either upper or lower, apply this equation: Axial point = mean of either the upper level or lower one $(Xm) \pm \alpha$ (Range between the upper level and lower one divided by2). Axial point = $Xm\pm$ α (Range/2) for the above experimental design.

3.7.1.2 Calculations for Upper and Lower axial points for experimental designs

There were different factors namely; pressure, number of plies and weight fraction which were considered. The upper and lower axial points were tabulated as shown in Table 3.2 below.

(a). Number of plies

Axial point = $Xm \pm \alpha$ (Range/2)

Axial point for plies $= 5 \pm 1.414\left(\frac{6-4}{2}\right)$

$$= 5 \pm 1.4142 * (1)$$

$$= 5 \pm 1.4142$$

The upper axial point for plies $= 5 + 1.4142 = 6.4142 \sim 6$

The lower axial point for plies $= 5 - 1.4142 = 3.59 \sim 4$

(b). Weight fraction (%)

Axial point for $W_f = 18 \pm 1.4142\left(\frac{23-13}{2}\right)$

$$= 18 \pm 1.4142 * (5)$$

$$= 18 \pm 7.071$$

The upper axial point for $W_f = 18 \pm 7.071 = 25.071\%$

The lower axial point for $W_f = 18 - 7.071 = 10.929\%$

The experiment designs had 13 runs as shown in table 3.4 below with coded values. The weight fraction (W_f) was determined from (Yogesha.B & Sanjay, 2018);

$$W_f = \frac{W_f}{W_f + W_m}$$

$$W_m = \frac{W_m}{W_f + W_m}$$

The volume fractions $V_f = \frac{{}^{Wf}/_{\rho f}}{{}^{Wf}/_{\rho f} + {}^{Wm}/_{\rho m}}$

Table 3. 3: Experimental design runs for two factors with actual values using central composite design

Runs	Plies	Fibre weight fraction (%)	Matrix w fraction and hardener (%)
1	6	13	87
2	5	18	82
3	4	23	77
4	6	18	82
5	6	23	77
6	5	18	82
7	4	13	87
8	5	18	82
9	5	18	82
10	5	25	75
11	4	18	82
12	5	11	89
13	5	18	82

3.8 DETERMINATION OF STATIC MECHANICAL PROPERTIES OF A COMPOSITE.

The static mechanical properties of the composites determined were tensile flexural and impact strengths.

3.8.1 Tensile strength

The composite samples were tested using universal testing machine (model Lancashire, UK; M/C Serial No:-500-10171. The tensile test was done according to ASTM D638 standard as shown in figure 3.11 below and figure 3.12 shows tensile samples before and after testing (Saiman et al., (2014), Sreenivasulu & Reddy, (2014), (Masood et al., 2018)

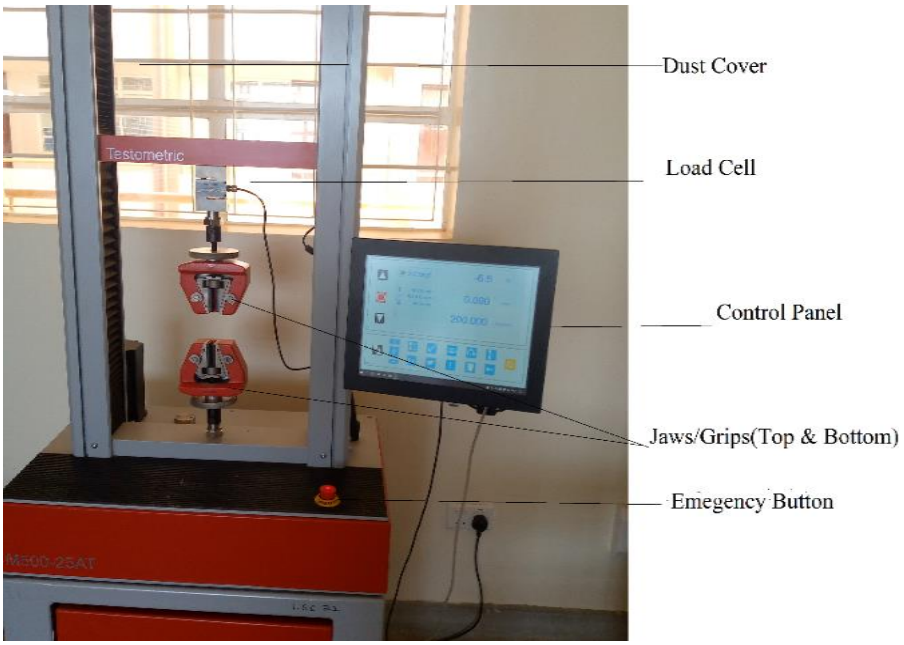

Figure 3.10 Universal Tensile machine (Testometric) with tensile testing jaws

Figure 3.11 Universal Tensile machine (Testometric) with tensile samples on the equipment.

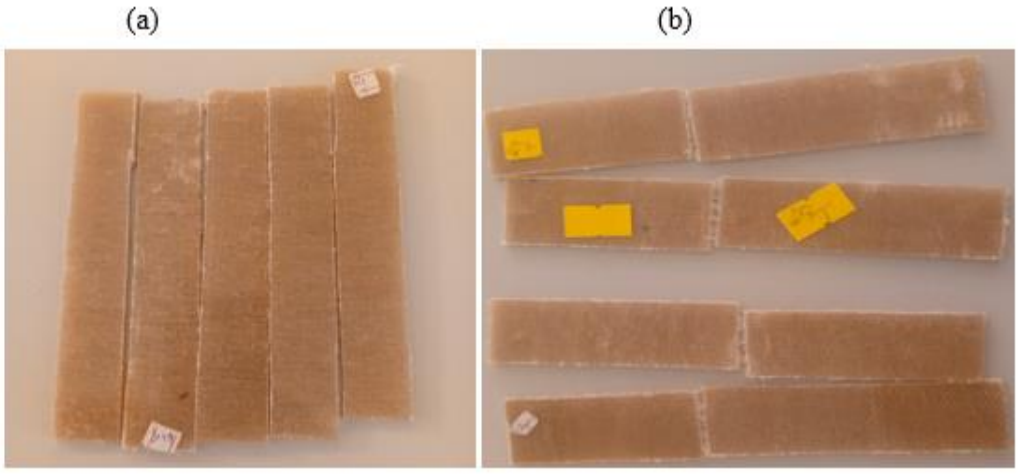

Figure 3. 12 : (a) before and (b) after testing tensile sample

3.8.2 Flexural strength test

The composite flexural strength was determined using a universal tensile tester model Lancashire, UK; M/C Serial No:-500-10171 according to ASTM D790 standard. A sample was cut and placed on the 3-point bending fixture. A load was applied on the middle of the

sample at 5mm/min head speed (Aisyah et al., 2018; Raju et al., 2012). Figure 3.14 shows the flexural testing with the jaws fixed and figure 3.15 shows flexural samples after testing.

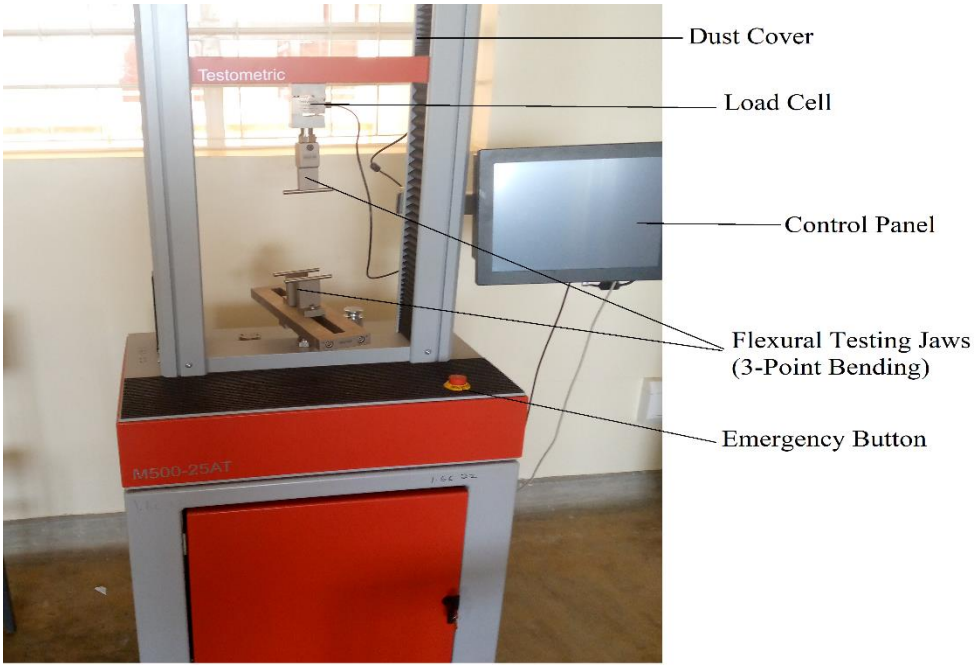

Figure 3. 13: Universal Tensile machine with Flexural testing jaws

Figure 3. 14 Universal Tensile machine with a flexural sample on the equipment.

Figure 3.15: Fractured flexural samples after testing

3.8.3 Impact strength test

Charpy impact test of the composite was performed on an impact testing machine (Model; Auto Impact-30, Maharashtra India, M/c Serial No. 10/2020-1585). A 60 x 10mm composite samples were prepared and cut according to ASTM D6110 – 10 as shown below in figure 3.17 (Shah et al., 2014; Susilowati & Sumardiyanto, 2018). The average of the results of five specimens tested was recorded. The impact strength was calculated as shown in equation 3.6;

$$a_{cU} = \frac{E}{h.b} * 10^3 \qquad \text{Equation 3.6}$$

Where,

h – Thickness (mm), a_{cU}-Impact strength of unnotched specimen (kJ/m^2) for Charpy test, E is the energy absorbed (J) by breaking the test and b – Width

Figure 3.16: Impact testing machine

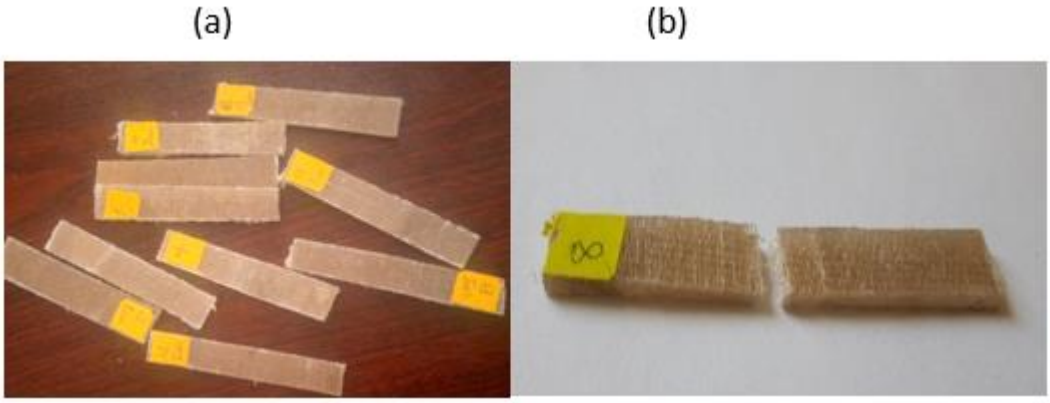

Figure 3.17: (a) before and (b) after testing impact samples.

3.9 DETERMINATION OF COMPOSITE THICKNESS

The composite thickness was established using a digital thickness gauge machine (Model YG141D; Hefei City, China: Fanyuan Instruments Co.,Ltd) as shown in figure 3.19. The

machine was set to zero before carrying out the test. Five readings each of the coated and uncoated specimens were recorded and the average value calculated.

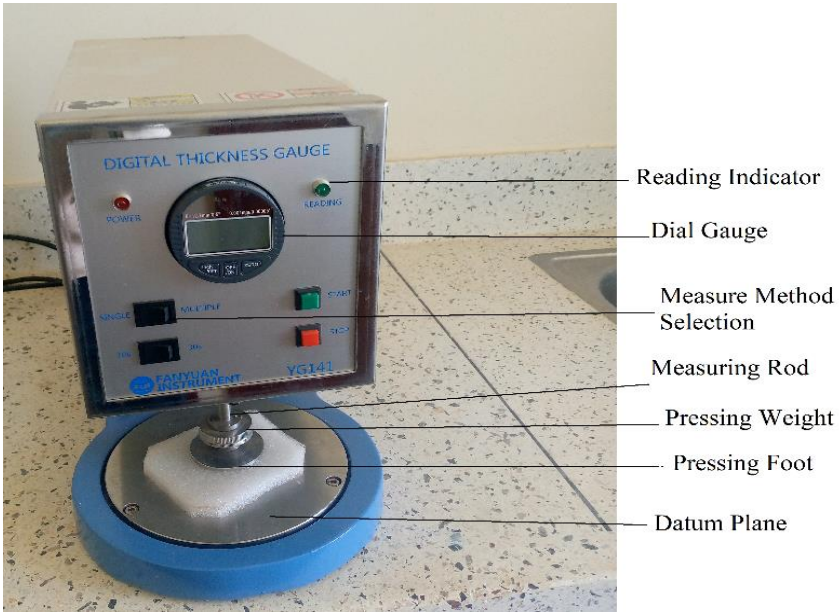

Figure 3.18 Showing composite thickness determination using a Digital thickness gauge machine in textile laboratory

CHAPTER 4: RESULTS AND DISCUSSION

4.1 Characterised properties of silk waste fabric

The results of the characterised properties of silk waste fabric are presented and discussed below.

4.1.1 Determination of wefts and warps

The wefts and warps/cm were determined by use of a pick glass and the results tabulated as shown in Table 4.1

Table 4. 1: Warps/wefts per inch of the fabric sample before degumming

Fabric direction	1st	2nd	3rd	4th	5th	6th	**Average**
Warps/inch	38	38	38	38	38	38	**38**
Wefts/inch	40	41	40	39	40	41	**40**

After the degumming process, the warp and weft density increased, by 1 and 4 warps and wefts per inch, respectively. Table 4.2 indicates the weft and warps per inch after degumming the fabric. This showed that the spaces between warps was less compared to those in wefts possibly because the beating up operation using a reed on the hand loom was done manually.

Table 4. 2: Warps/wefts per inch of the fabric sample after degumming

Fabric direction	1st	2nd	3rd	4th	5th	6th	**average**
Warps/inch	39	39	39	40	38	39	**39**
Wefts/inch	44	43	43	45	45	45	**44**

4.1.2 Measurement of tensile strengths of silk fabric

The measured values of the tensile strengths of silk waste fabrics are as shown in table 4.3 below. The mean value of the ten specimens tested was 16.80 MPa.

Table 4. 3 Showing tensile strengths s for silk samples

Sample	Maximum load (N)	Elongation (mm)	Tensile Strength (MPa)
1	100.30	10.64	17.06
2	95.60	11.26	15.30
3	149.40	14.07	23.90
4	85.30	11.21	13.65
5	86.20	8.39	13.79
6	106.6	10.52	17.06
7	116.00	9.27	18.56
8	103.20	9.52	16.51
9	96.30	10.11	15.41
10	104.50	12.64	16.72
Average	104.34	10.76	16.80

The load was for tensile considered in warp wise direction of the silk fabric, only warp yarns were drawn. While the load strain on tensile was seen in figure 4.1. The change of value of pick densities to the load-strain in the end direction ensued a mean stress at peak of 16.80

MPa elongation before failure. The outcome for elongation at maximum for warp course at 10.76 mm elongation before failure (Nasrun et al., 2016).

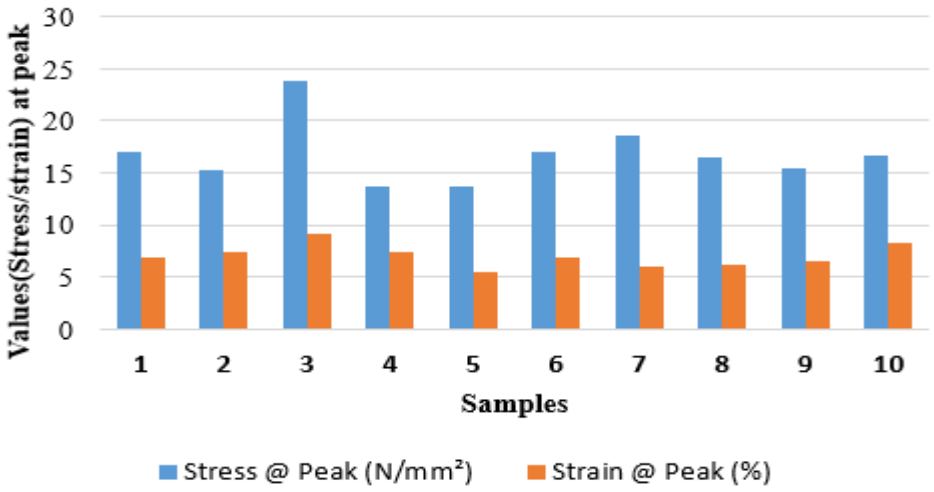

Figure 4. 1 Showing stress and strain values for silk samples

4.1.3 Measurement of fabric density

The average value of the weight for the ten samples was 0.30g. This value was small compared to the length used because the yarns which were used to weave the fabric were single yarns. The average thickness of the fabric was 0.4 mm and the grams per square metre (GSM) of the fabric was determined as 76.

4.2 MEASUREMENT OF COMPOSITE THICKNESS

Treated composites were denoted as T_t and non-treated as T_n. As depicted in Table 4.4, the values of thickness for non-treated samples are slightly higher than those of treated samples. This suggests a better adhesion between reinforcement and resin for the treated composites. When treating fibres with nanoparticles, the fibre inter molecular spaces largely open

(Nsengiyumva et al., 2021), hence allowing more chemicals to enter the openings easily. This results in good bonding between the resin and fibres and consequently reduced thickness of the treated samples (Davallo et al., 2010).

Table 4. 4 Composite thickness for both non-treated and treated composites

Run	Average thickness (mm)	
	Non-treated (T_n)	Treated (T_t)
1.	5.4	5.10
2.	2.9	2.55
3.	1.9	1.90
4.	3.3	3.06
5.	3.3	3.20
6.	2.9	2.66
7.	2.8	2.70
8.	2.9	2.56
9.	2.9	2.50
10.	2.3	2.10
11.	2.0	1.90
12.	4.8	4.50
13.	2.9	2.50

4.3 Determination of the static mechanical properties of bio-composite

4.3.1 Composite tensile strength

The values of Tensile strength of the non-treated silk waste fabric polyester composites at different fibre weight fractions and number of plies were as shown in table 4.5.

Table 4. 5: Tensile strength of the non-treated silk waste fabric polyester composites at different fibre weight fractions and number of plies

Fibre weight	Plies	Thickness (mm)	Cross-sectional area	Max. load (N)	Tensile Strength (MPa)
11wf%	5	4.8	120	1007.4	8.4
13wf%	6	5.4	135	1572.14	11.65
	4	2.8	70	871.88	12.46
18wf%	5	2.9	72.5	1405.2	19.38
	6	3.3	82.5	1435.76	17.4
	5	2.9	72.5	1258.72	17.36
	5	2.9	72.5	1282.52	17.69
	5	2.9	72.5	1408.58	19.43
	4	2	50	848.25	16.97
	5	2.9	72.5	1363.95	18.81
23wf%	4	1.9	47.5	816.08	17.18
	6	3.3	82.5	1592.74	19.31
25wf%	5	2.3	57.5	1184.8	20.61

The values of tensile strengths for non-treated samples for tensile composite were as shown in Table 4.5. The highest tensile strength of the sample before fracture (Tensile strength) was 20.61 MPa at 25% fibre weight fraction with five plies and the least value of tensile strength was obtained at 11wt% as 8.4 MPa.

Table 4. 6: Tensile strength of the non-treated silk waste fabric polyester composites at different fibre weight fractions

Fibre weight	Thickness (mm)	Cross-sectional area	Max. load (N)	Tensile strength (MPa)
11	4.8	120	1007.4	8.4
13	4.1	102.5	1222.0	12.1
18	2.8	70.7	1286.1	18.1
23	2.6	65.0	1204.4	18.2
25	2.3	57.5	1184.8	20.6

Figure 4.2 represents the tensile strengths of non-treated silk-polyester composites with of fibre weight fraction. The increase in fibre weight increased tensile strength up to 25wt% with the highest value of tensile strength recorded. The sample at 11wt.% showed the lowest value of tensile strength of 8.4 MPa.

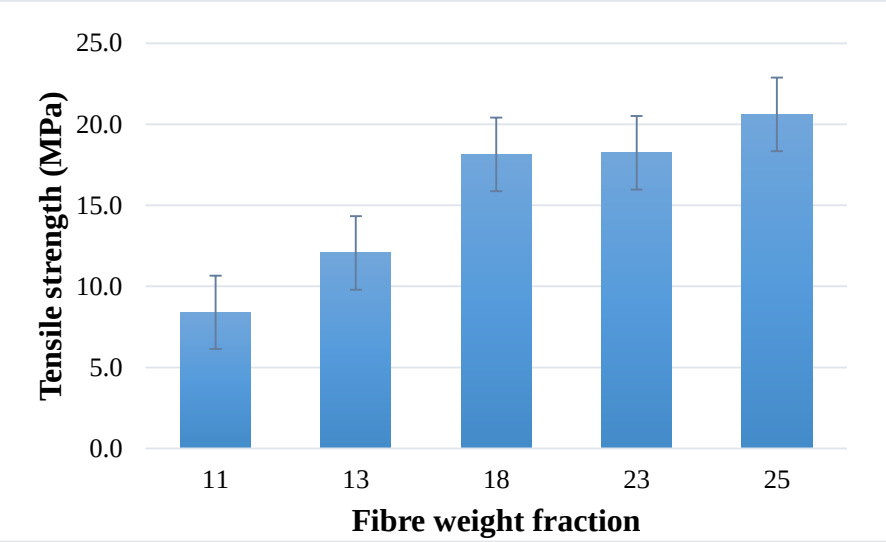

Figure 4. 2: Shows tensile strength of non-treated composites with fibre weight fraction

The table 4.7 indicates tensile strength of non-treated silk waste fabric polyester composites at different number of plies from 4-6. Five plies recorded the highest value of tensile strength.

Table 4. 7Tensile strength of non-treated silk waste fabric polyester composites at different number of plies

Plies	Thickness (mm)	Cross-sectional area	Max. load (N)	Tensile strength (MPa)
4	2.2	55.8	845.4	15.5
5	3.1	70.0	1273.0	17.4
6	4.35	108.75	1582.44	15.48

Figure 4.3 represents tensile strength of non-treated composites with number of plies. The increase in number of plies increased tensile strength up to 5 plies and further decreased on tensile strength with 6 plies. The five plies indicated as an optimum number of plies which showed the highest value of tensile strength beyond which the tensile strength of composites decreased.

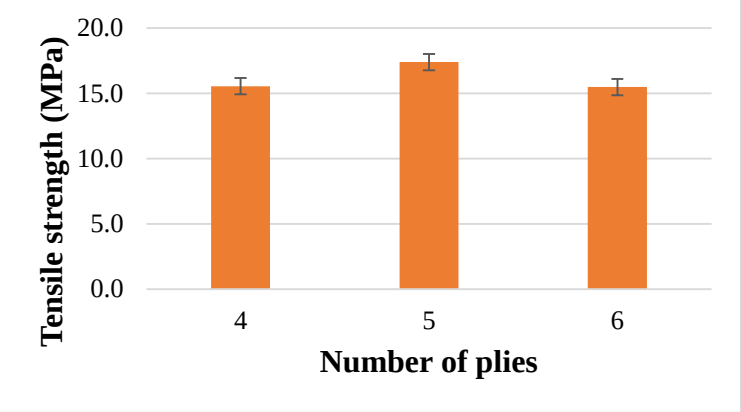

Figure 4. 3: Shows tensile strength of non-treated composites with number of plies

4.4.2 Composite flexural strength

The flexural strengths of non-treated composites with both different fibre weight fraction and plies were as shown in table 4.8.

The highest flexural strength for non-treated flexural composites was 52.13 MPa at 25wt.% for sample of five plies. The lowest flexural strength was 27.02 MPa for the sample with five plies at 11wt.%. Table 4.8 indicates the summary of the flexural strengths of non-treated silk fabric polyester composites at both different fibre weight fractions and plies.

Table 4. 8: Flexural strength of the non-treated silk waste fabric polyester composites at different fibre weight fractions and number of plies

Fibre weight	Plies	Thickness (mm)	Span length (mm)	Width (mm)	Max load (N)	Flexural Strength (MPa)
11	5	4.8	76.8	19	91.2	27.02
13	6	5.4	86.4	21	185.7	39.12
	4	2.8	44.8	11	28.62	21.9
	6	3.3	52.8	13	52.06	28.68
	5	2.9	46.4	11	41.54	30.98
18	5	2.9	46.4	11	55.72	41.56
	5	2.9	46.4	11	57.74	43.07
	4	2	32	8	19.8	29.7
	5	2.9	46.4	11	60.52	45.14
	5	2.9	46.4	11	47.28	35.26
23	4	1.9	30.4	7	21.12	37.61
	6	3.3	52.8	13	72.82	40.12
25	5	2.3	36.8	9	45.96	52.13

Table 4. 9: Flexural strength of the non-treated silk waste fabric polyester composites at different fibre weight fractions

Fibre weight	Thickness (mm)	Span length (mm)	Width (mm)	Max load (N)	Flexural Strength (MPa)
11	4.8	76.8	19.0	91.2	27.02
13	4.1	65.6	16.0	107.2	30.51
18	2.8	45.3	10.9	47.8	36.34
23	2.6	41.6	10.0	47.0	38.87
25	2.3	36.8	9.0	46.0	52.13

From figure 4.4, the highest flexural strength was 52.13 MPa at 25wt.% for a sample of five plies. The lowest flexural strength was 27.02 MPa for the sample with five plies at 11wt.%. This indicates that an increase in fibre weight fraction increased flexural strength and its highest value at 25wt%.

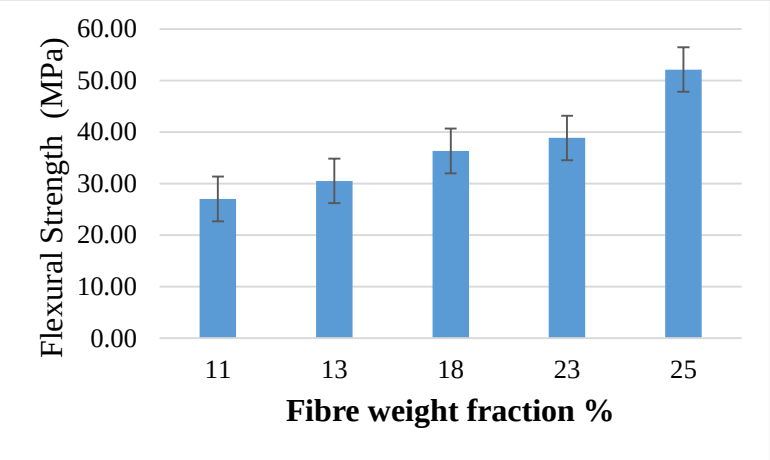

Figure 4. 4: Shows flexural strength of non-treated composites with fibre weight fraction

Table 4. 10: Flexural strength of the non-treated silk waste fabric polyester composites at different number of plies

Plies	Thickness (mm)	Span length (mm)	Width (mm)	Max load (N)	Flexural Strength (MPa)
4	2.2	35.7	8.7	23.2	29.7
5	3.2	51.5	12.3	59.0	37.2
6	4.0	64.0	15.7	103.5	36.0

Figure 4.5 represents flexural strength of non-treated composites with number of plies. The increase in number of plies increased flexural strength up to 5 plies and further decreased with 6 plies. The five plies indicated as an optimum number of plies which showed the

highest value of flexural strength beyond which the value of flexural strength slightly reduced.

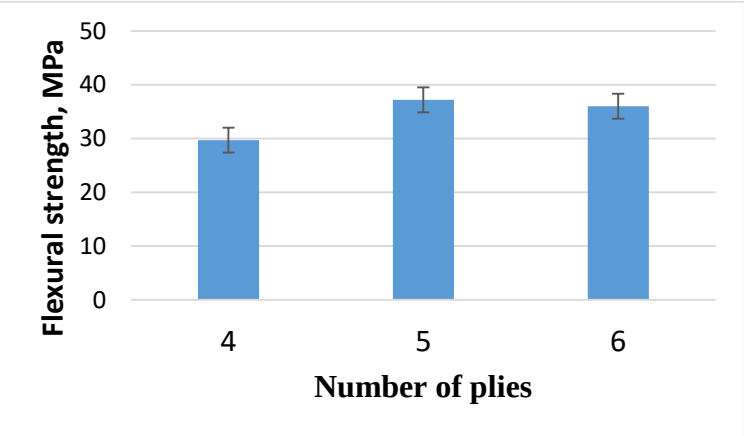

Figure 4. 5: Shows flexural strength of non-treated composites with number of plies

4.4.3 Impact strength of uncoated silk fabric composites.

The impact strength of non-treated silk fabric polyester composites at different fibre weight fractions and number of plies is summarized in Table 4.11.

Table 4. 11: Impact strength of the non-treated silk waste fabric polyester composites at different fibre weight fractions and number of plies

Fibre weight	Thickness	Plies	Width (mm)	Area, mm2	Absorbed energy, J	Impact energy, kJ/m2
11%	4.8	5	10	48	1.04	21.67
13%	5.4	6	10	54	1.11	20.56
	2.8	4	10	28	0.7	25
	2.9	5	10	29	0.72	24.83
18%	3.3	6	10	33	0.92	27.88
	2.9	5	10	29	0.72	24.83
	2.9	5	10	29	0.72	24.83

	2.9	5	10	29	0.72	24.83
	2	4	10	20	0.36	18
	2.9	5	10	29	0.72	24.83
23%	1.9	4	10	19	0.42	22.11
	3.3	6	10	33	0.88	26.67
25%	2.3	5	10	23	0.74	32.17

As would be expected, the 25% fibre weight fraction composites depicted the highest impact strength of 32.17 kJ/m^2 and 11wt% with the lowest impact strength of 21.67kJ/m^2

Table 4. 12: Impact strength of the non-treated silk waste fabric polyester composites at different fibre weight fractions

Fibre weight	Thickness	Width (mm)	Area, mm2	Absorbed energy, J	Impact energy, kJ/m2
11	4.8	10	48.0	1.04	21.67
13	4.1	10	41.0	0.91	22.78
18	2.8	10	28.3	0.70	24.29
23	2.6	10	26.0	0.65	24.39
25	2.3	10	23.0	0.74	32.17

Figure 4.6 represents impact strength of non-treated composites with number of plies. The increase in number of plies increased impact strength up to 5 plies and further decreased with 6 plies. The five plies indicated as an optimum number of plies which showed the highest value of impact strength beyond which the value of impact strength slightly reduced.

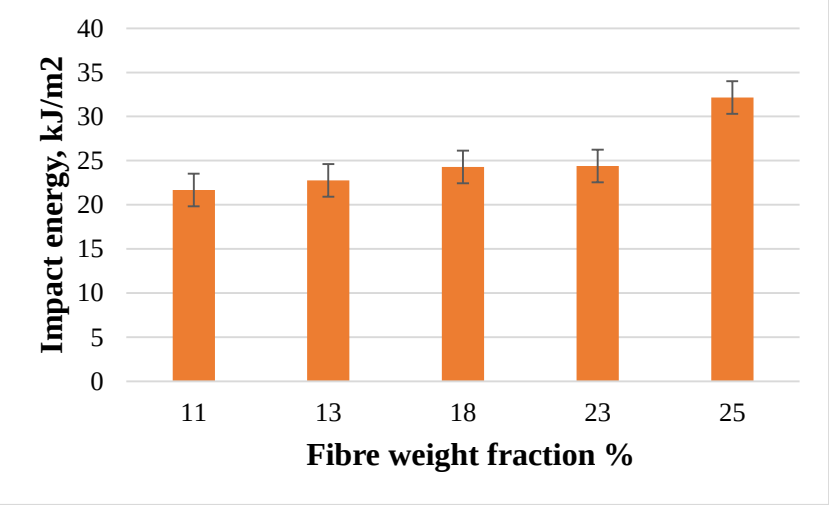

Figure 4. 6: Shows impact strength for the non-treated composites

Table 4. 13: Impact strength of the non-treated silk waste fabric polyester composites at different number of plies

Plies	Width (mm)	Area, mm2	Absorbed energy, J	Impact energy, kJ/m2
4	10	22.33	0.49	21.70
5	10	30.86	0.77	25.43
6	10	40.00	0.97	25.04

Figure 4.7 represents impact strength of non-treated composites with number of plies. The increase in number of plies increased impact strength up to 5 plies and further decreased with 6 plies. The five plies indicated as an optimum number of plies which showed the highest value of impact strength beyond which the value of impact strength slightly reduced.

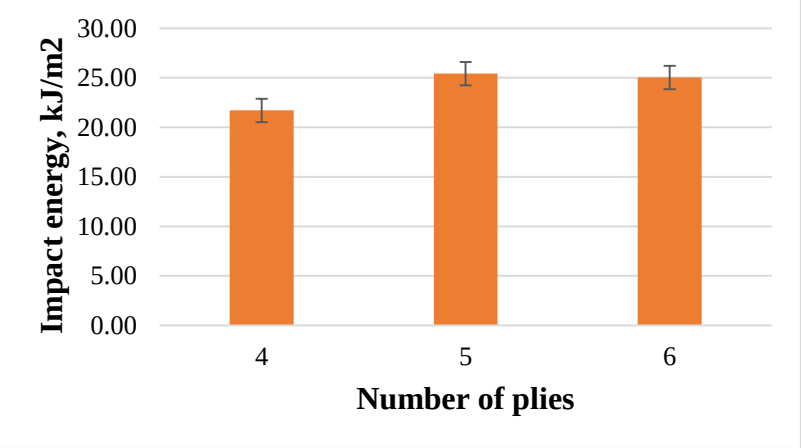

Figure 4. 7: Shows impact strength for non-treated composites with number of plies

4.5 Effect of ZnO nanoparticles on the mechanical properties of the silk waste polyester composites

4.5.1 Effect on the tensile strength

The values of tensile strengths for treated samples were obtained and tabulated as shown in Table 4.14. For treated composites the tensile strength greatly increased with the nanoparticles treatment for both number of plies and fibre weight fraction compared to non-treated composites.

Table 4. 14: Tensile strength of the treated silk waste fabric polyester composites at different fibre weight fractions and number of plies

Fibre weight	Plies	Thickness (mm)	Cross-sectional area (mm^2)	Max. load (N)	Tensile strength (MPa)
11wf%	5	4.5	112.5	1639.05	14.57
13wf%	6	5.1	127.5	2003.9	15.72
	4	2.7	67.5	1049.15	15.54
18% wf	5	2.6	63.8	1244.66	19.52
	6	3.1	76.5	1389.5	18.16

	5	2.6	63.8	1162.44	18.22
	5	2.6	64	1289.47	20.15
	5	2.5	62.5	1235.06	19.76
	4	1.9	47.5	795.63	16.75
	5	2.5	62.5	1241.7	19.79
23wf %	4	1.9	47.5	1012.4	19.89
	6	3.2	80	1474.16	18.43
25wf%	5	2.1	52.5	1116.99	21.68

For example, a sample with 5piles and 25% weight fabric fraction showed the highest values that is 21.68 MPa, compared to the value of 20.61 MPa when non-treated. The average the tensile strengths of the treated composites were higher than those of non-treated composites. The treatment increased tensile strengths as shown in table 4.15.

Table 4. 15: Tensile strength of the treated silk waste fabric polyester composites at different fibre weight fractions

Fibre weight	Thickness (mm)	Cross-sectional area (mm^2)	Max. load (N)	Tensile strength (MPa)
11	4.5	112.5	1639.1	14.57
13	3.9	97.5	1526.5	15.63
18	2.5	62.9	1194.1	18.9
23	2.6	63.8	1243.3	19.2
25	2.1	52.5	1117.0	21.7

Figure 4.8 represents the effect of fibre weight fraction on the tensile strengths of treated composites. It can be seen that the tensile strength of the coated composites increased with increasing number of plies up to 5 and weight fraction up to 25wt%.

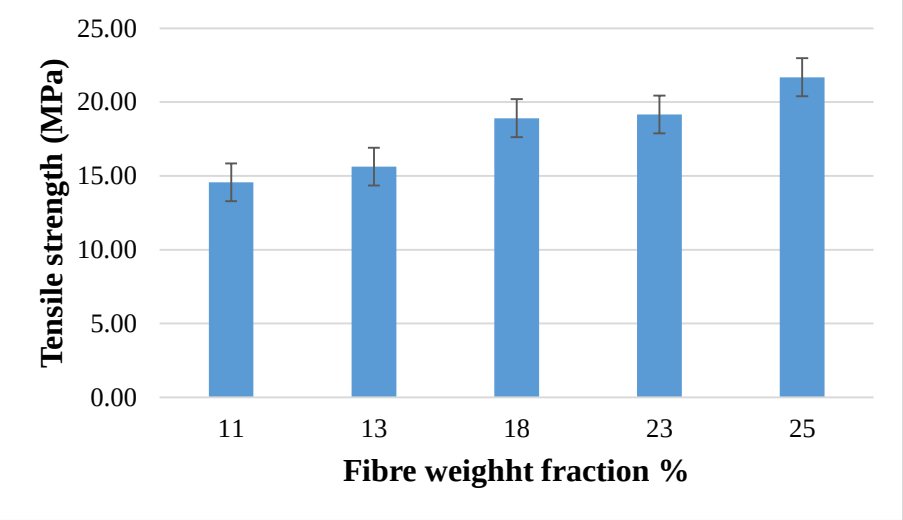

Figure 4. 8: Effect of fibre weight fraction on the tensile strength of coated composites

Table 4. 16: Tensile strength of the treated silk waste fabric polyester composites at different number of plies

Plies	Thickness (mm)	Cross-sectional area	Max. load (N)	Tensile strength (MPa)
4	2.3	57.5	922.39	16.15
5	2.8	69.6	1273.32	18.92
6	3.8	94.7	1622.52	17.44

Figure 4.9 shows the increase in number of plies up to 5 plies of treated silk waste fabric composites increased the tensile strength and the optimum value as 5 plies. It indicated the maximum value of 18.92 MPa compared to non-treated of 17.4 MPa. The increase on tensile was due to the treatment with nanoparticles.

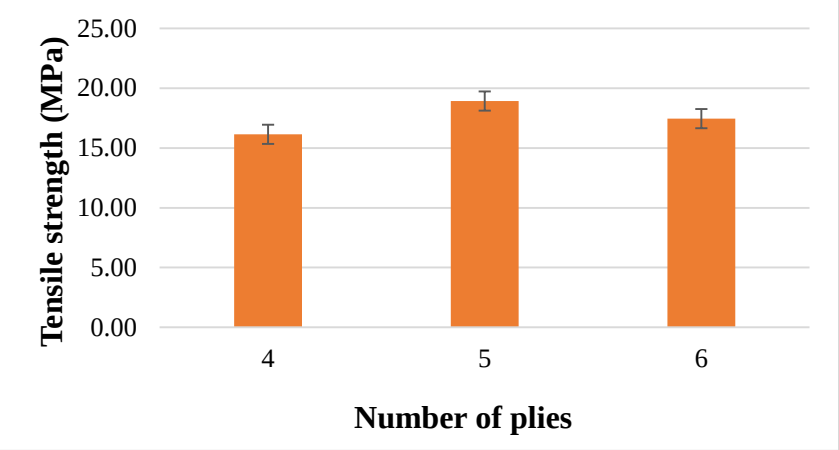

Figure 4. 9: Effect of number of plies on the tensile strength of coated composites

4.5.2 Effect on the flexural strength

Table 4.17 indicates flexural strength of the treated silk waste fabric polyester composites at different fibre weight fractions and number of plies

Table 4. 17: Flexural strength of the treated silk waste fabric polyester composites at different fibre weight fractions and number of plies

Fibre weight	Plies	Thickness (mm)	Span length (mm)	Width (mm)	Max load (N)	Flexural Strength (MPa)
11	5	4.5	72	18	128.9	38.19
13	6	5.1	81.6	20.4	219.8	48.9
	4	2.7	43.2	10.8	39.68	32.65
18	6	3.1	49	12.24	59	34.9
	5	2.6	40.8	10.2	61.8	50.71
	5	2.6	40.8	10.2	45.04	47.04
	5	2.6	41	10.24	54.75	50.13
	4	1.9	30.4	7.6	22.64	39.65
	5	2.5	40	10	52.58	50.48
	5	2.5	40	10	52.63	50.52
23	4	1.9	30.4	7.6	24.81	41.23

	6	3.2	51.2	10.8	74.84	51.97
25	5	2.1	33.6	8.4	39.3	53.47

After treating silk waste fabric with zinc oxide nanoparticles, the highest flexural strength of the samples treated was 53.47 MPa for sample with five plies at 25wt%. The lowest flexural strength was 38.19 MPa with five plies at 11wt.% with as indicated in table 4.18. This generally showed that the coating of silk fabric samples with ZnO NPs positively affected the adhesion between reinforcement and matrix hence the increase in flexural strength. This was in line with the finding of Wang et al., (2015) that treating fibres with nanoparticles enhanced the mechanical properties.

Table 4. 18: Flexural strength of the treated silk waste fabric polyester composites at different fibre weight fractions

Fibre weight	Thickness (mm)	Span length (mm)	Width (mm)	Max load (N)	Flexural Strength (MPa)
11	4.5	72.0	18	128.9	38.19
13	3.9	62.4	16	129.7	40.78
18	2.5	40.3	10	49.8	46.20
23	2.6	40.8	9	49.8	46.60
25	2.1	33.6	8	39.3	53.47

Figure 4.6 shows the effect of fibre weight fraction on the flexural strength of treated composites. The highest flexural strength of the samples treated was 53.47 MPa at 25wt%. Increase on fibre weight fraction increased the flexural strength.

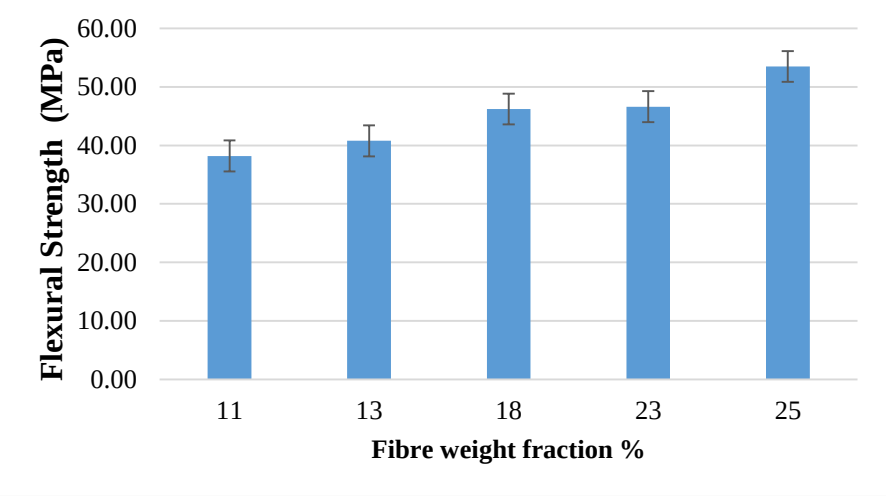

Figure 4. 10: Effect of fibre weight fraction on the flexural strength of coated composites

Table 4.19 indicates flexural strength of the treated silk waste fabric polyester composites at different number of plies

Table 4. 19: Flexural strength of the treated silk waste fabric polyester composites at different number of plies

Plies	Thickness (mm)	Span length (mm)	Width (mm)	Max load (N)	Flexural Strength (MPa)
4	2.2	34.7	8.7	29.0	37.8
5	2.8	44.0	11.0	62.1	48.6
6	3.8	60.6	14.5	117.9	45.3

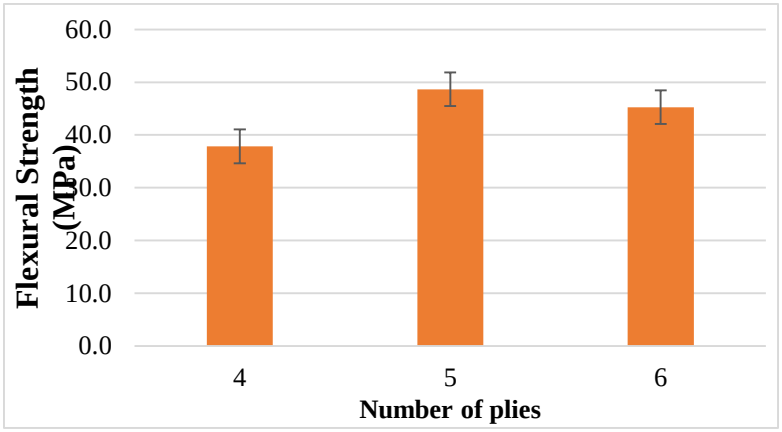

Figure 4. 11: Effect of number of plies on the flexural strength of coated composites

4.6 ANOVA with regression models

Experiments were designed and conducted to evaluate the effect of plies and fibre weight fraction on the mechanical properties of silk fabric reinforced polyester composite. The results for experiments showed in Tab. 4.20 are for three responses; tensile strength, flexural strength and impact strength. The respective response ANOVA details are given in Tables 4.21 and 4.22.

Table 4. 20 CCD experimental design matrix and experimental responses.

Runs	Factors		Responses				
			Uncoated			Coated	
	A	B	Y_1	Y_2	Y_3	Y_{1C}	Y_{2C}
	Plies	Fibre weight fraction (%)	Tensile strength (Mpa)	Flexural strength (Mpa)	Impact strength (Kj/m^2)	Tensile strength (Mpa)	Flexural strength (Mpa)
1	5	18	19.38	35.26	24.83	20.15	50.52
2	5	18	17.36	30.98	24.83	19.79	50.71
3	4	18	16.97	29.70	18.00	21.28	39.65
4	5	11	8.4	27.02	21.67	14.57	38.19
5	4	13	12.46	21.90	12.86	15.54	32.65
6	6	23	19.31	40.12	30.91	18.43	48.56

7	4	23	17.18	37.61	22.11	17.89	41.23
8	5	18	17.69	45.14	24.83	19.76	50.48
9	6	13	11.65	39.12	20.56	15.72	48.90
10	5	25	20.61	52.13	32.17	21.68	53.47
11	5	18	19.43	41.56	24.83	19.52	50.87
12	5	18	19.13	43.07	24.83	20.16	50.13
13	6	18	17.40	28.68	27.88	18.16	34.90

4.6.1 Uncoated composite

With respect to the statistical analysis, the coefficient of determination, employed to fit the models for tensile, flexural and impact strength were 0.9495, 0.7688 and 0.9182 respectively obtained from ANOVA which implies that the models are significant and satisfactory fits to the experimental data. It was established that the relationships between tensile, flexural and impact strength with the input variables of plies and weight fraction accounted for the data variability satisfactorily. Higher values of coefficient of determination (close to 1/100%) indicate more significance of the model to predict the respective responses. The polynomial regression models which relate the tensile strength (Y_1), flexural strength (Y_2) and impact strength (Y_3) with the variables (plies (P) and fibre weight fraction (W)) was determined using Minitab software version 17 and represented in the equations 4.1, 4.2 and 4.3

$Y_1 = -33.6 + 6.41\ P + 3.207\ W - 0.881\ P^2 - 0.0889\ W^2 + 0.147\ PW$ ……Equation 4.1

$Y_2 = -181.7 + 64.8\ P + 4.60\ W - 4.93\ P^2 + 0.0105\ W^2 - 0.735\ PW$ ……Equation 4.2

$Y_3 = -46.4 + 20.57\ P + 0.28W - 1.775\ P^2 + 0.0086\ W^2 + 0.055\ PW$…….Equation 4.3

The significance of the quadratic models was also determined by evaluating the F-values (the Fisher's F-test) which were expressed as the square to residual error ratio of the mean model. The respective F-values for tensile, flexural and impact strengths were 26.34, 10.58 and 205.62 accompanied by low probability values ($p < 0.05$). Additionally, model significance

was depicted by non-significant values (F- and p-values) of lack of fit test of 0.376, 0.491 and 0.714 for tensile, flexural and impact strengths respectively. Table 4.16 details the F-values and their respective p-values for the models and their respective terms.

Table 4. 21: ANOVA for responses of uncoated composites

Source	DF	Adj SS	Adj MS	F-value	P-value	R^2	Remark
Tensile strength							
Model	5	149.298	29.860	26.34	0.000	0.9495	Significant
Linear	2	110.339	55.170	48.66	0.000		Significant
P	1	0.468	0.468	96.91	0.541		Non-Significant
W	1	109.872	109.872	16.23	0.000		Significant
Square	2	36.805	18.403	9.05	0.002		Significant
P^2	1	5.397	5.397	4.76	0.065		Non-Significant
W^2	1	34.333	34.333	30.28	0.001		Significant
2-way interaction	1	2.154	2.154	1.90	0.211		Non-Significant
PW	1	2.154	2.154	1.90	0.211		Non-Significant
Error	7	7.937	1.134				
Lack-of-fit	3	4.000	1.333	1.35	0.376		Non-Significant
Pure Error	4	3.937	0.984				
Total	12	157.235					
Flexural strength							
Model	5	611.535	122.307	10.58	0.023	0.7688	Significant
Linear	2	382.648	191.324	5.60	0.035		Significant
P	1	41.814	41.814	1.22	0.305		Non-Significant
W	1	340.833	340.833	9.97	0.016		Significant
Square	2	174.821	87.410	2.56	0.147		Non-Significant
P^2	1	169.021	169.021	4.95	0.062		Non-Significant
W^2	1	0.479	0.479	0.01	0.909		Non-Significant
2-way interaction	1	54.067	54.067	1.58	0.249		Non-Significant
PW	1	54.067	54.067	1.58	0.249		Non-Significant
Error	7	100.375	34.169				
Lack-of-fit	3	93.42	31.14	0.96	0.491		Non-Significant
Pure Error	4	138.810	34.703				
Total	12	850.720					
Impact strength							
Model	5	288.05	57.60	205.62	0.001	0.9182	Significant
Linear	2	264.41	132.20	36.06	0.000		Significant
P	1	116.07	116.07	31.66	0.001		Significant
W	1	148.34	148.34	40.46	0.000		Significant
Square	2	24.23	11.66	3.18	0.104		Non-Significant
P^2	1	21.91	21.91	5.88	0.044		Significant

W^2	1	0.32	0.32	0.09	0.776	Non-Significant
2-way interaction	1	0.30	0.30	0.08	0.782	Non-Significant
PW	1	0.30	0.30	0.08	0.782	Non-Significant
Error	7	25.66	3.66			
Lack-of-fit	3	25.66	8.55	0.64	0.714	Non-Significant
Pure Error	4	0.16	0.02			
Total	12	313.710				

The 3-D surface response plots these models were presented in figure 4.7. The optimum operating values of the factors are the targets of using response surface method. The graphical illustration portrayed possible interaction effects between the two variables. The 3-D plots show the effect of number of plies and fibre weight fraction on the respective selected mechanical properties of the composite.

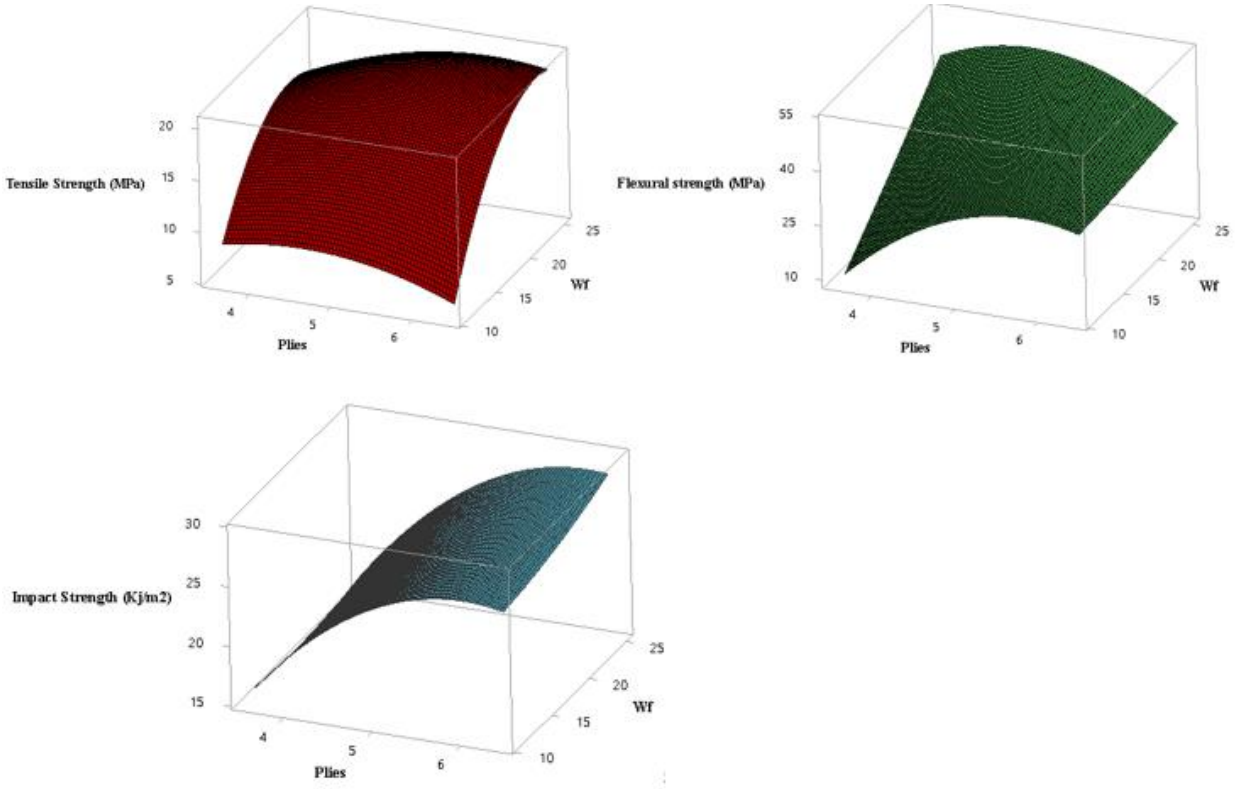

Figure 4. 12 Response surface plots for responses of uncoated composites

4.6.2 Coated composite

As a remarkable approach of data analysis, ANOVA has been used to establish the significance of model terms in assessing the mechanical properties of the fibre reinforced composites through analyzing the probability values (P-values) and variance value (F-ratio). Higher F-values and low P-values indicate more effectiveness of the model terms. P-values lower than 0.05 display the good implication of the input factors, thereby failing to accept the null hypothesis.

According to Table 4.22 and the earlier mentioned explanation with respect to P-values, the model terms, including linear, square and interactions sign significantly affect the tensile strength (Y_{1C}) and flexural strength (Y_{2C}) of the composite. The following second-order polynomial models have been established through the ANOVA of the material properties with respect to their significant terms.

$$Y_{1C} = -15.5 + 5.05\,P + 2.28\,W - 0.584\,P^2 - 0.0553\,W^2 + 0.018\,PW \quad \text{.....Equation 4.4}$$

$$Y_{2C} = -197.7 + 73.2\,P + 5.91\,W - 6.31\,P^2 - 0.0814\,W^2 - 0.446\,PW \quad \text{.....Equation 4.5}$$

Coefficients of determination (R^2) were determined to check the model fitness. R^2 was 0.7501 and 0.7636 for tensile strength and flexural strength correspondingly. This implies that 75.01% and 76.36% of the variation in the respective mechanical properties can be explained by the models. High coefficient of determination value indicates better correlation between the actual and the predicted values.

Adequacy of the models was as well evaluated by the lack of fit test. Lack of fit indicates the variation of the data around the model being fitted and it would be significant if the model does not fit the data well. Non-significant lack of fit, however, is good because the model is geared towards perfect fitness. It implied that a good correlation between the factors and responses could be drawn by the developed models. The suggested models for tensile strength and flexural strength can therefore, be used to pilot into design space to determine the optimum points.

Table 4.22: ANOVA analysis for responses of coated composites

Source	DF	Adj SS	Adj MS	F-value	P-value	R^2	Remark
Tensile strength							
Model	5	44.7114	8.9423	5.20	0.044	0.7501	Significant
Linear	2	30.2234	15.1117	7.10	0.021		Significant
P	1	1.70333	1.70333	0.80	0.401		Non-Significant
W	1	28.5201	28.5201	13.41	0.008		Significant
Square	2	14.4550	7.2275	3.30	0.093		Non-Significant
P^2	1	2.3745	2.3745	1.12	0.326		Non-Significant
W^2	1	13.3006	13.3006	6.25	0.041		Significant
2-way interaction	1	0.0329	0.0329	0.02	0.904		Non-Significant
PW	1	0.0329	0.0329	0.02	0.904		Non-Significant
Error	7	14.8926	2.1275				
Lack-of-fit	3	14.5976	4.8659	2.45	0.167		Non-Significant
Pure Error	4	0.2950	0,0738				
Total	12	59.6040					
Flexural strength							
Model	5	454.280	90.856	18.06	0.002	0.7636	Significant
Linear	2	3885.99	113.33	17.67	0.004		Significant
P	1	439.55	439.55	22.32	0.058		Non-Significant
W	1	626.53	626.53	4.97	0.015		Significant
Square	2	224.21	19074	13.02	0.020		Significant
P^2	1	88.15	88.15	13.23	0.003		Significant
W^2	1	3.41	3.41	1.82	0.069		Non-Significant
2-way interaction	1	102.82	34.27	0.99	0.353		Non-Significant
PW	1	89.40	89.40	0.99	0.353		Non-Significant
Error	7	9.25	1.52				
Lack-of-fit	3	9.370	1.87	1.67	0.076		Non-Significant
Pure Error	4	1.870	0.37				
Total	12	594.897					

Three-dimensional surface plots were plotted to further understand the fitted model. The surface plots suggest that the linear and interaction terms plus the quadratic term explain just about all of the variability in the tensile strength (Y_{1C}) and flexural strength (Y_{2C}). The need

for a quadratic term in each factor was mandatory as dictated from the fold in the surface (Figure 4.13) on each factor. The purpose of these plots is to simultaneously create understanding of the main effects and interactions among the factors for the selected response.

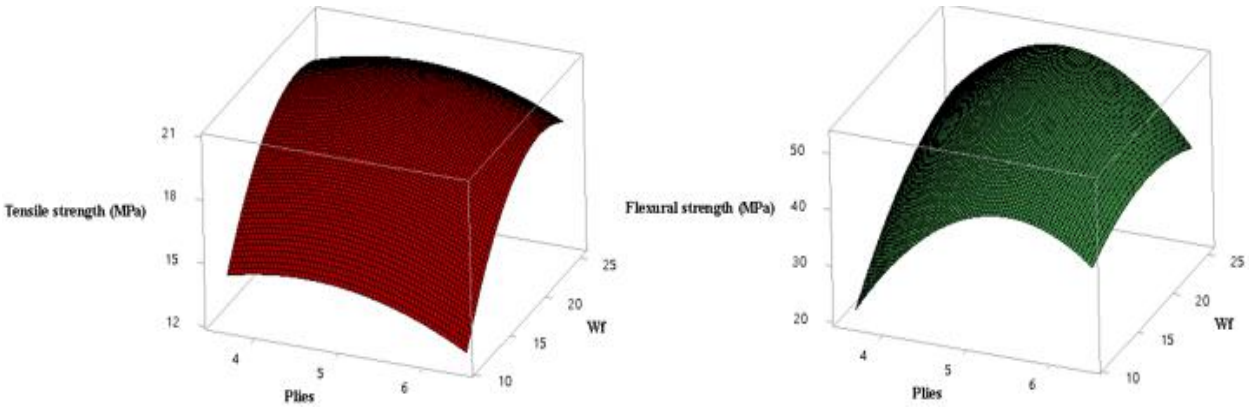

Figure 4. 13 Response surface plots for responses of coated responses

Increase in number of plies does not demonstrate a significant effect on tensile strength though it gradually decreases tensile strength and sharply increases flexural up to 5 plies and thereafter, it decreases gradually for both mechanical properties as illustrated in figure 4.13. On the other hand, tensile strength decreases with increase in fibre weight fraction up to 20% followed by a gradual increase giving a small interaction between the plies and weight fraction. However, the increase in weight fraction increases flexural strength up-to about 5 plies. Beyond 5 plies, the increase in weight fraction gradually reduces the flexural strength.

4.6.3 Optimization

Optimal points for the selected mechanical properties of silk fabric reinforced polyester composite were established to attain the maximum tensile strength and flexural strength. The

second order polynomial models developed in this analysis were utilized for each of the responses in demand to obtain specific optimum input factors. Response optimizer with composite desirability in Minitab software version 17 was employed for the multi-response optimization exercise. The optimum tensile strength (Y_1) and flexural strength (Y_2) of 20.5273 and 52.1703 MPa was obtained at the number of plies of 4.9571 (~5) and at the fibre weight fraction of 24.76175 (~25) with a composite disability of 0.8867. Figure 4.14 illustrates the optimized input conditions for the tensile and flexural strength properties of silk fabric reinforced polyester composite.

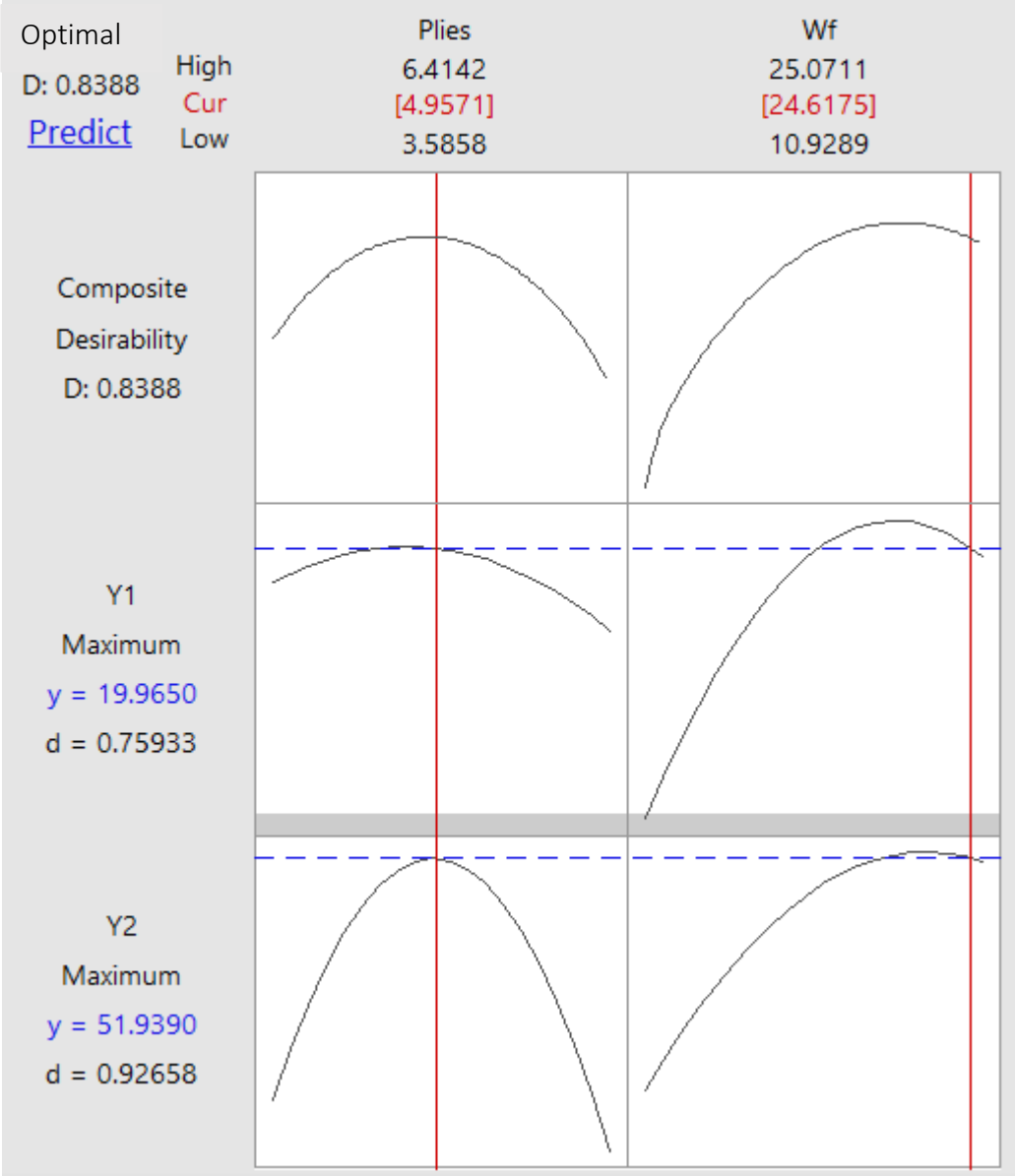

Figure 4.14: Optimization plots

4.7 PRODUCT CHARACTERISATION

4.7.1 SEM Morphological properties

In figure 4.15 c) and d), the SEM images indicate that the Zinc oxide nanoparticles were deposited on the surface of the fabric. When comparing figure 4.15 a) and b) the surfaces were seen with no particles which indicates that there is no deposition (Majumder et al., 2020).

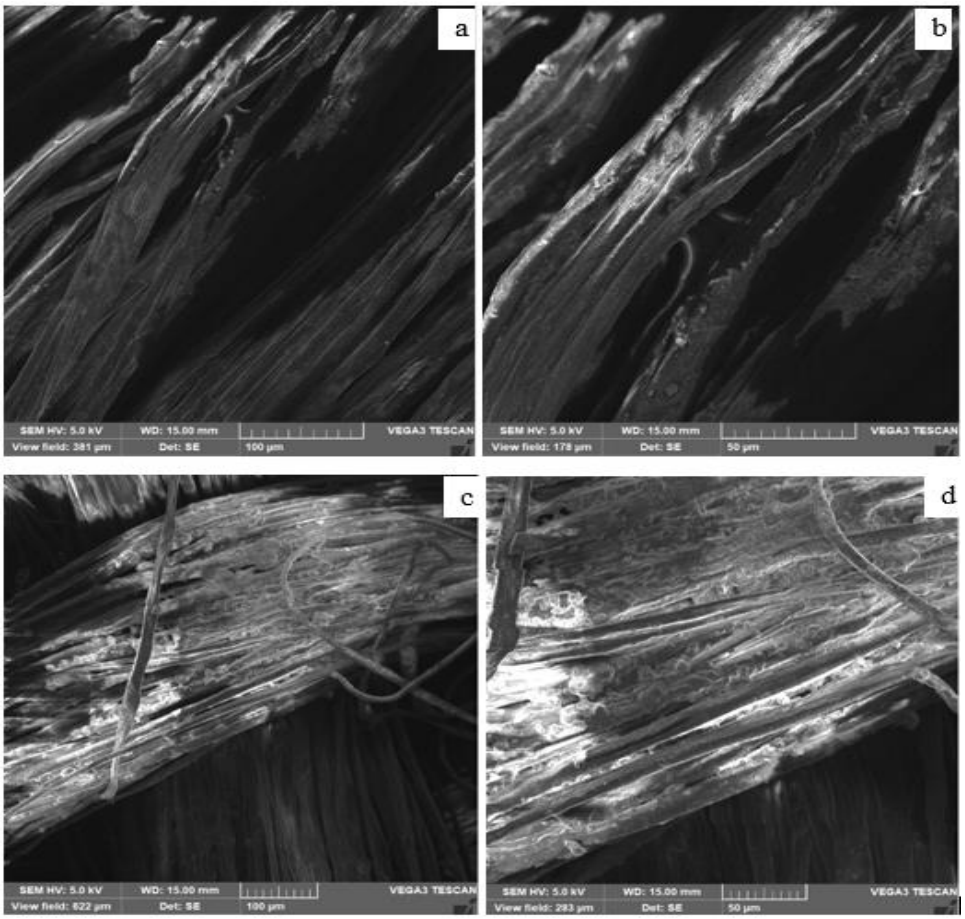

Figure 4.15: SEM images for silk waste fabric (a) and (b) non-treated and (c) and (d) treated silk at 100 and 50 magnification.

Non treated composites showed low resin penetration on the silk fibres thus implying poor impregnation of the fibres by the resin (Saiman et al., 2014) as shown in figure 4.16 (a) and (b). Images are representatives along the longitudinal fractured region of the tensile samples obtained at 100 and 50 magnification respectively. Similarly in figure 4.16 (c) and (d) are representatives along the fractured longitudinal region obtained at the same magnification for treated tensile fractured composites. Many silk fibres have been pulled out and appear without resin. Voids occurrence was higher in figure 4.16 (a) and (b). Thus a weak silk fiber/matrix adhesion is expected due to the incompatibility between hydrophobicity of the polyester resin and the hydrophilicity of untreated silk fibers (Hamidi et al., 2018), (Kim et al., 2006). A good wetting of the silk fibres and less pullout effect were observed in figures 4. 16 (c) and (d) due to high compatibility between treated fibres and the resin. Thus less pullout effect was seen in these figures.

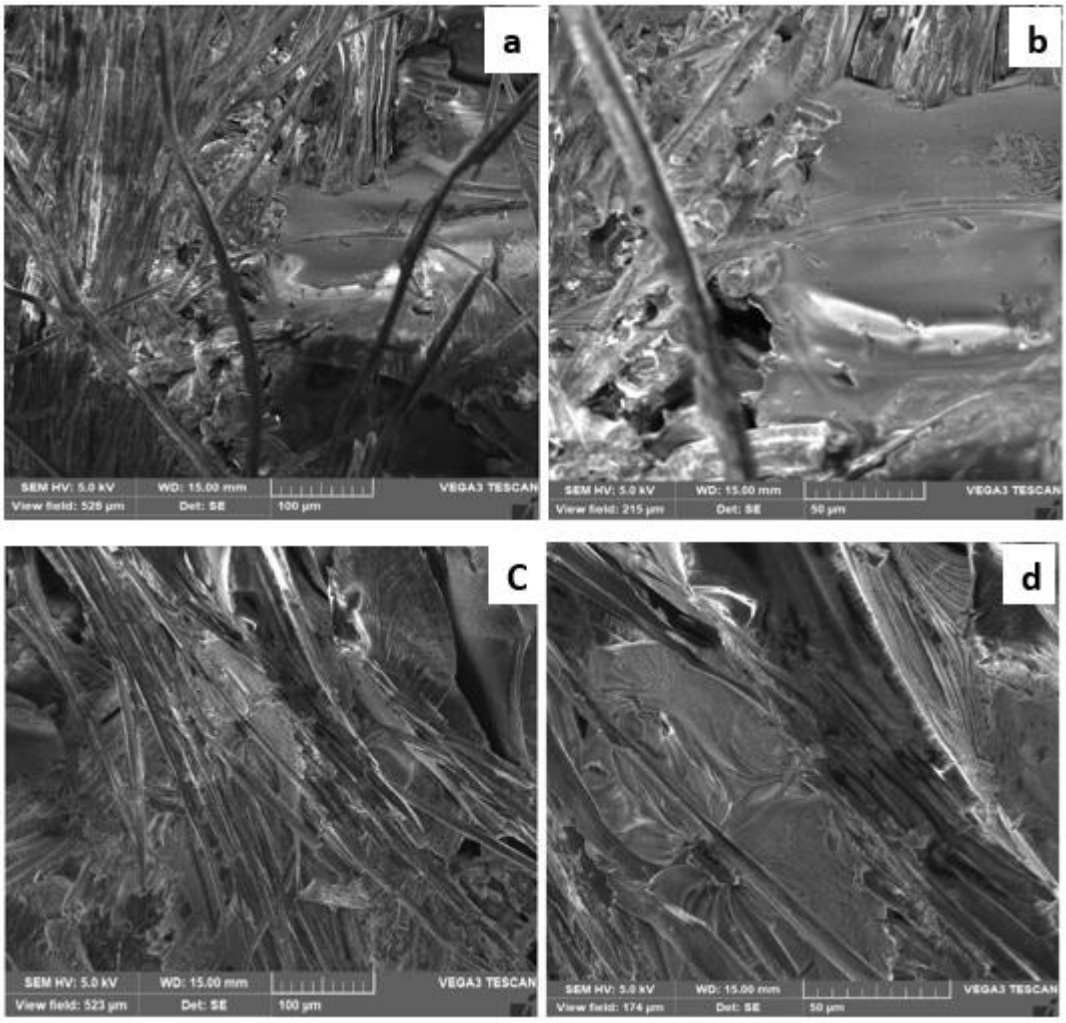

Figure 4.16: SEM images of fractured surfaces of non-treated and treated composites after tensile test at 400x (a, c) and 1000x (b, d) magnification

Impact strength of a composite is a measure of the ability of the material to resist the fracture failure under stress applied at high speed and is directly related to the toughness of the material. This effect is due to poor adhesion between fabrics and matrix (Venkata Reddy et al., 2008)

Figures 4.17 (a, b, c and d) are SEM images of the fractured region of the composite samples under impact obtained at $1mm, 200um,$ 100um and 50um respectively.

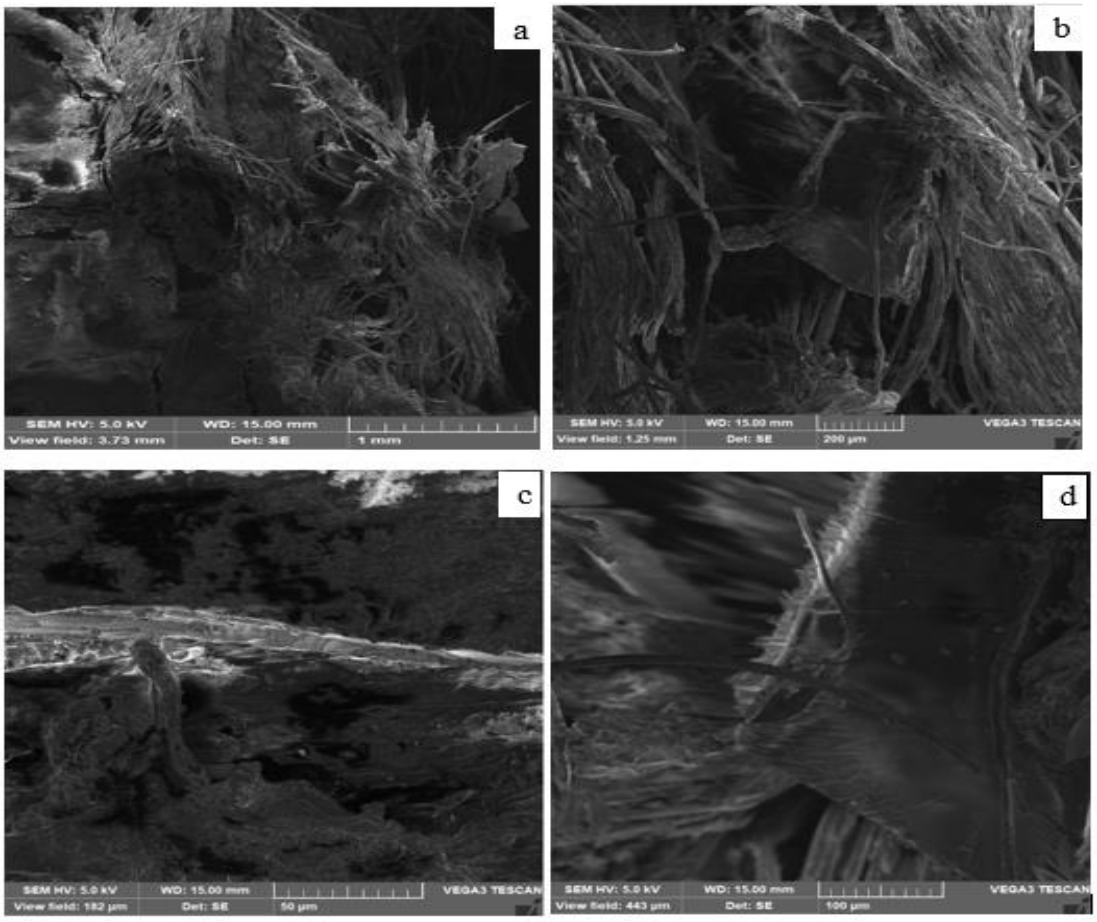

Figure 4.17: SEM images of fractured composite surfaces after impact test a) 1mm, b) 200µm, c) 50µm and d)100µm magnification

In figure 4.18 SEM images show impregnation of fibres with resin was high due to the incompatibility between hydrophobicity of the polyester resin and the hydrophilicity of untreated silk fibers (Hamidi et al., 2018). A poor wetting of the silk fibres and more pullout

effect were observed in figures 4.18 (c) and (d) due to low compatibility between treated fibres and resin.

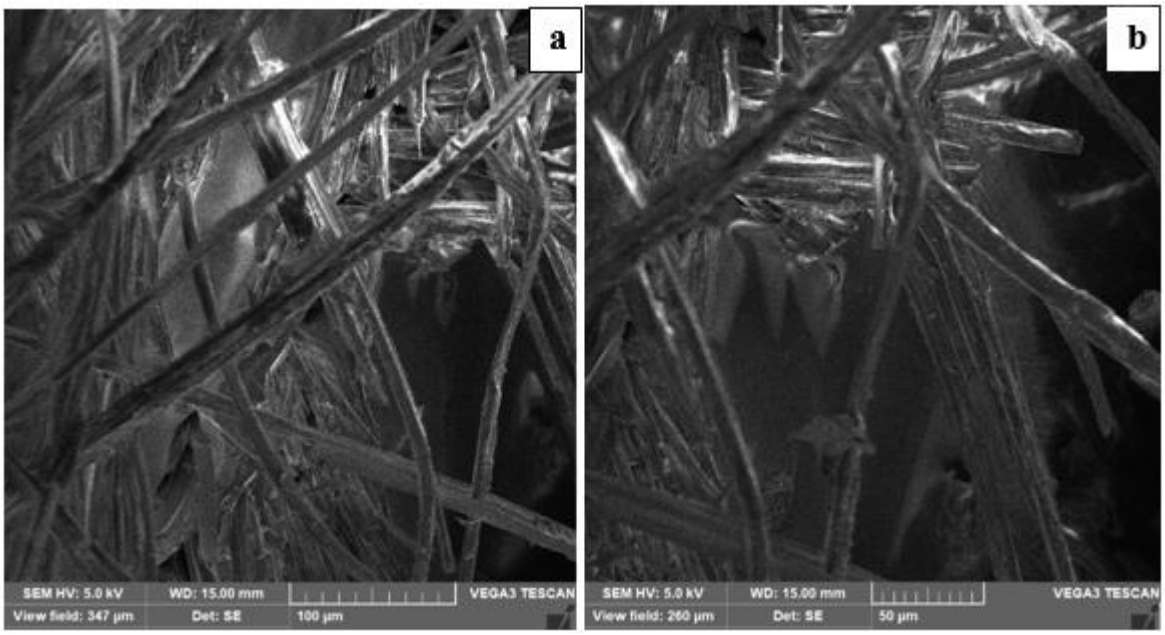

Figure 4.18: SEM images of fractured surface of untreated composites after flexural test at a) 100µm and b) 50µm

The silk/polyester interface was investigated by the use of SEM under careful review to examine the composites crosswise. The review showed an extensive debonding on the silk/polyester composites indicating weak compatibility between fibre and matrix along the longitudinal direction. A weak fiber/matrix adhesion is expected due to the incompatibility between the hydrophilicity of untreated silk fibers and the hydrophobicity of unsaturated polyester resin.

4.7.2 FTIR analysis

The spectrum in figure 4.19 indicate the peaks at 1750cm^{-1} to 720cm^{-1} as the highest in accordance to the spectra of extending vibration band of C=O at 1732cm^{-1} and C–O–C

stretching vibration band at 1071cm^{-1} and 1267cm^{-1}, these being attributed to the presence of ester groups in polyester resin. The peak at the region of 723cm^{-1} is for aromatic (C-H). The spectrum at 2979cm^{-1} indicates the carboxylic group (-COOH) (Hardy et al., 2016), (Majumder et al., 2020). The band at 625cm^{-1} corresponds to the combination of ZnO nanoparticles and Polyester in the treated composites (Majumder et al., 2020), (Nourbakhsh et al., 2018). The treated and non-treated composites showed the peaks shifting from 2979cm^{-1} to 2956cm^{-1} which showed chemical bonding between the resin and silk fibres (J. Wang et al., 2018).

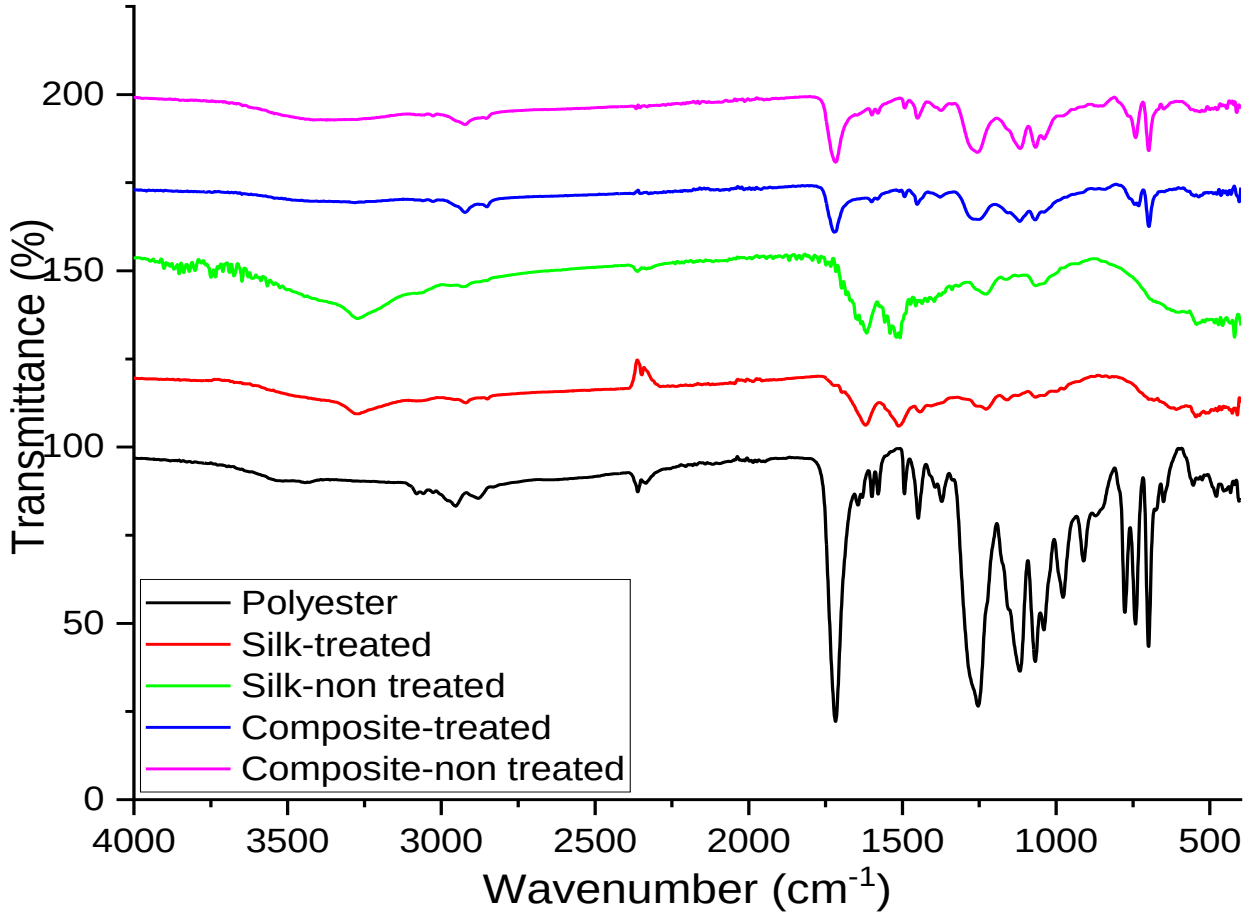

Figure 4.19: FTIR results for polyester, treated and non-treated silk and composites

4.7.3 TGA

Figure 4.20 shows TGA thermograms of unsaturated polyester resin, silk fabric treated and untreated and composite treated and untreated. The weight of polyester was practically constant below 250^0C (Hamidi et al., 2018). Thermal degradation indicates three major steps. The first before degradation occurred where the weight was fairly stable between 30-250^0C due to the impurities and moisture contact present with approximately 10% weight loss. The second step began with the decomposition of organic constituents of the silk and composites between 300 and 400^0C. The weight losses of approximately 35%, 30%, 20%, 15% and -15% of silk non-treated, silk treated, composited treated, and composite untreated and polyester resin respectively. The third step up to 700^0C, the weight loss was observed to be minimal. The treated composite sample was more thermally stable than non-treated composites. Thermal stability of polyester was enhanced by inclusion of silk and it was higher for treated silk composite (Gheno et al., 2015), (Kim et al., 2006).

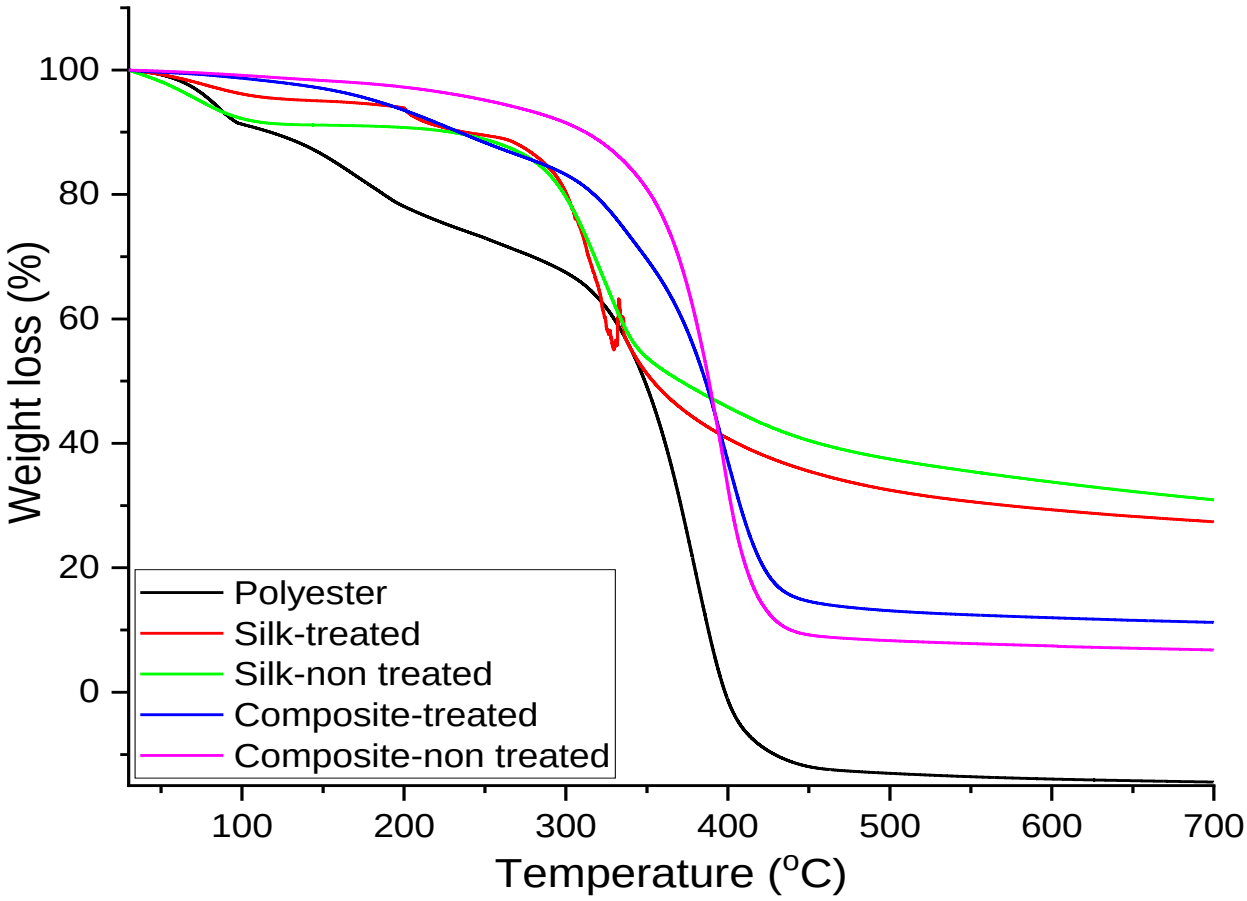

Figure 4.20: TG curves for polyester, treated and non-treated silk and composites at 10^0C/min

CHAPTER 5: CONCLUSION AND RECOMMENDATIONS

5.1 CONCLUSIONS

The current study aimed at analysing the mechanical (tensile, flexural and impact), thermal and morphological properties of bio-composites from unsaturated resin reinforced with silk waste fabric (treated and non-treated) composites. Bio-composites both treated with zinc oxide nanoparticles and non-treated were produced by a consolidation pressure of 2.65 kN/m^2. Central composite design was used in the design of experiments and the fibre weight fraction was varied from 11 to 25% and number of plies from 4-6. The following conclusions were drawn from this study.

a). The tensile properties of silk waste fabric showed an average value of 16.8 MPa in warp wise direction.

b). Fabrication of the ZnO nanoparticle coated silk waste fabric bio-composite showed smaller thickness of the composites in comparison with non-treated composites. This is attributed to the treatment with nanoparticles for further opening of interfacial spaces in the silk waste fabric.

c). Bio-composites produced from non-treated silk waste fabric showed the optimum tensile, flexural and impact strengths at 25% fibre weight fraction. Similarly, bio-composites produced from non-treated silk waste fabric showed the optimum tensile, flexural and impact strengths at 5 plies.

d). Bio-composites produced from treated silk waste fabric showed better mechanical properties of tensile and flexural strengths than similar bio-composites at the same fibre weight fraction of 25%. Bio-composites produced from treated silk waste fabric

showed better mechanical properties of tensile and flexural strengths than similar bio-composites at 5 plies. This generally showed that the coating of silk fabric samples with ZnO NPs enhanced the adhesion between reinforcement and matrix resulting in an increase on the static mechanical properties. An increase on the tensile strength and flexural strength of the silk waste fabric composite samples was obtained as 23.6% and 24.9% respectively with zinc oxide nanoparticles treatment.

e). Treated fractured tensile composites had less debonding and pullout effects than non-treated composites under SEM analysis. Thermal stability of polyester was stable by inclusion of silk and more thermally stable for treated silk composites on thermal analysis.

5.2 RECOMMENDATIONS

The study recommended future research studies on increasing the number of plies with orientation at angle and establish their effect on mechanical and thermal properties and morphology.

The study recommended future research works on the use of thermal evaporation technique onto silk waste fabric instead of pad dry cure method which is commonly used and analysis of the effect of the technique on mechanical and thermal properties of the composites.

Finally, Nanoparticles synthesized from plants could be studied to establish their effect on the mechanical and thermal properties and morphology of the bio-composites

REFERENCES

Aisyah, H. A., Paridah, M. T., Khalina, A., Sapuan, S. M., Wahab, M. S., Berkalp, O. B., Lee, C. H., & Lee, S. H. (2018). Effects of fabric counts and weave designs on the properties of LaminatedWoven Kenaf/Carbon fibre reinforced epoxy hybrid composites. *Polymers*, *10*(12). https://doi.org/10.3390/polym10121320

Aisyah, H. A., Paridah, M. T., Sapuan, S. M., Ilyas, R. A., Khalina, A., Nurazzi, N. M., Lee, S. H., & Lee, C. H. (2021). A comprehensive review on advanced sustainable woven natural fibre polymer composites. *Polymers*, *13*(3), 1–45. https://doi.org/10.3390/polym13030471

Allam, O. G. (2011). Improving Functional Characteristics of Wool and Some Synthetic Fibres. *Open Journal of Organic Polymer Materials*, *01*(01), 8–19. https://doi.org/10.4236/ojopm.2011.11002

Arakem, D., Sinézio, J., & Campos, D. C. (2017). CORONA TREATMENT APPLIED IN THE PROCESSING OF SILK WASTE . STUDY OF PROPERTIES SUCH AS HYDROPHILICITY AND TENSILE STRENGTH . *Procedia Engineering*, *200*, 18–25. https://doi.org/10.1016/j.proeng.2017.07.004

Azam, M., Jahanzaib, M., & Wasim, A. (2014). *Surface roughness modeling using RSM for HSLA steel by coated carbide tools*. *December*. https://doi.org/10.1007/s00170-014-6707-5

Banga, H., Singh, V. K., & Choudhary, S. K. (2015). *Fabrication and Study of Mechanical Properties of Bamboo Fibre Reinforced Bio-Composites*. *6*(1), 84–99.

Bhatia, S. (2016). Natural polymer drug delivery systems: Nanoparticles, plants, and algae. In *Natural Polymer Drug Delivery Systems: Nanoparticles, Plants, and Algae*.

https://doi.org/10.1007/978-3-319-41129-3

Bhatt, A. T., Gohil1, P. P., & Chaudhary, V. (2018). Primary Manufacturing Processes for Fiber Reinforced Composites: History, Development & Future Research Trends. *IOP Conference Series: Materials Science and Engineering*, *330*(1). https://doi.org/10.1088/1757-899X/330/1/012107

Bhatt, P. (2011). *A STUDY ON DYEING PERFORMANCE ON MULBERRY SILK WASTE / WOOL BLENDED FABRIC Thesis Department of Clothing and Textiles © PUNJAB AGRICULTURAL UNIVERSITY*.

Buhr, E., Senftleben, N., Klein, T., Bergmann, D., Gnieser, D., Frase, C. G., & Bosse, H. (2009). Characterization of nanoparticles by scanning electron microscopy in transmission mode. *Measurement Science and Technology*, *20*(8). https://doi.org/10.1088/0957-0233/20/8/084025

Cheung, H.-Y., Lau, K.-T., Ho, M.-P., & Mosallam, A. (2009). Study on the Mechanical Properties of Different Silkworm Silk Fibers. *Journal of Composite Materials*, *43*(22), 2521–2531. https://doi.org/10.1177/0021998309345347

Cheung, Yan, H., Lau, K. T., Tao, X. M., & Hui, D. (2008). A potential material for tissue engineering: Silkworm silk/PLA biocomposite. *Composites Part B: Engineering*, *39*(6), 1026–1033. https://doi.org/10.1016/j.compositesb.2007.11.009

Darshan, S. M., Suresha, B., & Divya, G. S. (2016). *Waste Silk Fiber Reinforced Polymer Matrix Composites: A Review*. 183–189.

Davallo, M., Pasdar, H., & Mohseni, M. (2010). Mechanical properties of unsaturated polyester resin. *International Journal of ChemTech Research*, *2*(4), 2113–2117.

Faruk, O., Bledzki, A. K., Fink, H., & Sain, M. (2013). *Progress Report on Natural Fiber*

Reinforced Composites. 1–18. https://doi.org/10.1002/mame.201300008

Fuqua, M. A., Huo, S., & Ulven, C. A. (2012). Natural fiber reinforced composites. *Polymer Reviews*, *52*(3–4), 259–320. https://doi.org/10.1080/15583724.2012.705409

Gashti, M. P., Alimohammadi, F., Song, G., & Kiumarsi, A. (2012). *Characterization of nanocomposite coatings on textiles : a brief review on Microscopic technology*. 1424–1437.

Gheno, G., Ganzerla, R., Bortoluzzi, M., & Paganica, R. (2015). Determination of degradation kinetics of two polyester thermosetting powder coatings using TGA and colorimetric analysis. *Progress in Organic Coatings*, *78*, 239–243. https://doi.org/10.1016/j.porgcoat.2014.08.015

Ghiasi, M., Naghashzargar, E., & Semnani, D. (2014). *Silk Fibroin Nano-Coated Textured Silk Yarn by Electrospinning Method for Silk Fibroin Nano-Coated Textured Silk Yarn by Electrospinning Method for Tendon and Ligament Scaffold Application*. *August*. https://doi.org/10.4028/www.scientific.net/NH.7.35

Govindaraju, R., & Jagannathan, S. (2018a). Optimization of mechanical properties of silk fiber-reinforced polypropylene composite using Box–Behnken experimental design. *Journal of Industrial Textiles*, *47*(5), 602–621. https://doi.org/10.1177/1528083716667257

Govindaraju, R., & Jagannathan, S. (2018b). *Optimization of mechanical properties of silk fiber-reinforced polypropylene composite using Box – Behnken experimental design*. https://doi.org/10.1177/1528083716667257

Hamidi, Y. K., Yalcinkaya, M. A., Guloglu, G. E., & Pishvar, M. (2018). *Silk as a Natural Reinforcement : Processing and Properties of Silk / Epoxy Composite Laminates*.

https://doi.org/10.3390/ma11112135

Hardy, J. G., Torres-Rendon, J. G., Leal-Egaña, A., Walther, A., Schlaad, H., Cölfen, H., & Scheibel, T. R. (2016). Biomineralization of engineered spider silk protein-based composite materials for bone tissue engineering. *Materials*, *9*(7). https://doi.org/10.3390/MA9070560

Hoang, M. D. (2015). *Procedure for Making Flat Thermoplastic Composite Plates by Automated Fiber Placement and Their Mechanical Properties*. *April*. https://doi.org/10.1017/CBO9781107415324.004

Ibrahim, I. D., Jamiru, T., Sadiku, E. R., Kupolati, W. K., Agwuncha, S. C., & Ekundayo, G. (2016). Mechanical properties of sisal fibre-reinforced polymer composites: A review. *Composite Interfaces*, *23*(1), 15–36. https://doi.org/10.1080/09276440.2016.1087247

Indran, S., & Raj, R. E. (2015). Characterization of new natural cellulosic fiber from Cissus quadrangularis stem. *Carbohydrate Polymers*, *117*, 392–399. https://doi.org/10.1016/j.carbpol.2014.09.072

Jabbar, A. (2017). *Characterization of Mechanical and Thermomechanical Behavior of Sustainable Composite Materials Based on Jute Dissertation*. https://doi.org/10.1353/csp.2012.0018

Javali, U. C., Padaki, N. V., Das, B., & Malali, K. B. (2015). Developments in the use of silk by-products and silk waste. In *Advances in Silk Science and Technology*. Elsevier Ltd. https://doi.org/10.1016/B978-1-78242-311-9.00013-6

Joshi, M., Bhattacharyya, A., & Ali, S. W. (2008). Characterization techniques for nanotechnology applications in textiles. *Indian Journal of Fibre and Textile Research*,

33(3), 304–317. https://doi.org/10.1039/c0cp00504e

Khan, M. R., Islam, A., Habib, A., & Pervez, N. (2015). *Raw-Silk-Processing-to-Textile-Fibre-and-Comparative-Analysis-between-Acid.docx. February 2016*.

Khanjani, S., Morsali, A., & Joo, S. W. (2013). In situ formation deposited ZnO nanoparticles on silk fabrics under ultrasound irradiation. *Ultrasonics Sonochemistry*, *20*(2), 734–739. https://doi.org/10.1016/j.ultsonch.2012.09.013

Kim, H. S., Park, B. H., Yoon, J., & Jin, H. J. (2006). The role of N-carboxymethylation of chitosan in the thermal stability and dynamic. *Polym Int*, *55*(November 2006), 961–969. https://doi.org/10.1002/pi

Li, L., & Hu, Z. (2006). Sericulture and silk production in China. *Indian Silk*, *45*(1).

Loreto, G., Leardini, L., Arboleda, D., & Nanni, A. (2014). Performance of RC Slab-Type Elements Strengthened with Fabric-Reinforced Cementitious-Matrix Composites. *Journal of Composites for Construction*, *18*(3), A4013003. https://doi.org/10.1061/(ASCE)CC.1943-5614.0000415

Majumder, S., Dahiya, U. R., Yadav, S., Sharma, P., Ghosh, D., Rao, G. K., Rawat, V., Kumar, G., Kumar, A., & Srivastava, C. M. (2020). Zinc oxide nanoparticles functionalized on hydrogel grafted silk fibroin fabrics as efficient composite dressing. *Biomolecules*, *10*(5). https://doi.org/10.3390/biom10050710

Masood, Z., Ahmad, S., Umair, M., Shaker, K., & Karahan, M. (2018). *Mechanical Behaviour of Hybrid Composites Developed from Textile Waste*. *1*(127), 46–52. https://doi.org/10.5604/01.3001.0010.7796

Mondal, I. H., Islam, K., & Islam, M. (2016). *Modification of Silk Fibres with Acetic Anhydride and Phthalic Anhydride-Effects on Dyeability and Physio-Chemical*

Properties. *5*(2), 25–30. https://doi.org/10.5923/j.textile.20160502.01

Murugan, R., Ramesh, R., & Padmanabhan, K. (2014). Investigation on Static and Dynamic Mechanical Properties of Epoxy Based Woven Fabric Glass / Carbon Hybrid Composite Laminates. *Procedia Engineering*, *97*, 459–468. https://doi.org/10.1016/j.proeng.2014.12.270

Nadiger, V. G., & Shukla, S. R. (2016). *Antibacterial properties of silk fabric treated with silver nanoparticles*. *5000*(January). https://doi.org/10.1080/00405000.2015.1129756

Nasrun, F. M. Z., Yahya, M. F., Ghani, S. A., & Ahmad, M. R. (2016). *Effect of weft density and yarn crimps towards tensile strength of 3D angle interlock woven fabric Effect of Weft Density and Yarn Crimps Towards Tensile Strength of 3D Angle Interlock Woven Fabric*. *020003*(October). https://doi.org/10.1063/1.4965051

Nevres, M. E. (2009). *Effects of processing parameters on the mechanical behavior of continuous glass fiber / polypropylene composites*.

Ninpetch, U., Tsukada, M., & Promboon, A. (2015). Mechanical properties of silk fabric degummed with bromelain. *Journal of Engineered Fibers and Fabrics*, *10*(3), 69–78. https://www.scopus.com/inward/record.uri?eid=2-s2.0-84940934600&partnerID=40&md5=8ed3d4e8e2688e6860ea4f28e7c0e7f3

Noorunnisa, KHANAM, REDDY, G. R., RAGHU, K., & NAIDU, S. V. (2010). *Tensile, Flexural, and Compressive Properties of Coir/Silk Fiber-reinforced Hybrid Composites*. *29*(14), 2124–2127. https://doi.org/10.1177/0731684409345413

Noorunnisa, P., REDDY, M. M., K. Raghu, K. J. A., & NAIDU*, S. V. (2007). *Tensile, Flexural and Compressive Properties of Sisal/Silk Hybrid Composites*. *26*(10). https://doi.org/10.1177/0731684407079347

Nourbakhsh, S., Montazer, M., & khandaghabadi, Z. (2018). Zinc oxide nano particles coating on polyester fabric functionalized through alkali treatment. *Journal of Industrial Textiles*, *47*(6), 1006–1023. https://doi.org/10.1177/1528083716657819

Nsengiyumva, W., Zhong, S., Lin, J., Zhang, Q., Zhong, J., & Huang, Y. (2021). Advances, limitations and prospects of nondestructive testing and evaluation of thick composites and sandwich structures: A state-of-the-art review. *Composite Structures*, *256*, 112951. https://doi.org/10.1016/j.compstruct.2020.112951

Ogunsile, B. O., & Oladeji, T. G. (2016). Utilization of banana stalk fiber as reinforcement in low density polyethylene composite. *Revista Materia*, *21*(4), 953–963. https://doi.org/10.1590/S1517-707620160004.0088

Parvinzadeh Gashti, M., Pakdel, E., & Alimohammadi, F. (2016). Nanotechnology-based coating techniques for smart textiles. In *Active Coatings for Smart Textiles* (Issue December). Elsevier Ltd. https://doi.org/10.1016/B978-0-08-100263-6.00011-3

Raju, G. U., Kumarappa, S., & Gaitonde, V. N. (2012). Mechanical and physical characterization of agricultural waste reinforced polymer composites. *Journal of Materials and Environmental Science*, *3*(5), 907–916.

Ramamoorthy, S. K., Skrifvars, M., & Persson, A. (2015). A review of natural fibers used in biocomposites: Plant, animal and regenerated cellulose fibers. *Polymer Reviews*, *55*(1), 107–162. https://doi.org/10.1080/15583724.2014.971124

Rani, K. V., Sarma, B., & Sarma, A. (2019). Plasma pretreatment on tasar silk fabrics coated with ZnO nanoparticles against antibacterial activity. *Surface Review and Letters*, *26*(5). https://doi.org/10.1142/S0218625X18501937

Ruoyuan, S. O. N. G., Haruhiro, I. N. O., & Teruo, K. I. (2009). *Mechanical Property of*

Silk / Bamboo Composite Paper for Effective Utilization of Waste Silk. *55*(3), 85–90.

Saiman, M. P., Wahab, M. S., & Wahit, M. U. (2014). The Effect of Fabric Weave on the Tensile Strength of Woven Kenaf Reinforced Unsaturated Polyester Composite. *Proceedings of the International Colloquium in Textile Engineering, Fashion, Apparel and Design 2014 (ICTEFAD 2014)*, 25–29. https://doi.org/10.1007/978-981-287-011-7_5

Saravana, B. D., & Mohan, K. G. C. (2013). Thermal Properties of Maize Fiber Reinforced Unsaturated Polyester Resin Composites. *Proceedings of the World Congress on Engineering*, *III*.

Selvaraj, D. E., Priyan, S. S., & Kumar, M. R. (2014). *Understanding the Basics of Nano Technology*. *3*(5), 130–136.

Shah, D. U., Porter, D., & Vollrath, F. (2014). Can silk become an effective reinforcing fibre ? A property comparison with flax and glass reinforced composites. *COMPOSITES SCIENCE AND TECHNOLOGY*, *101*, 173–183. https://doi.org/10.1016/j.compscitech.2014.07.015

Shahidi, S., Wiener, J., & Ghoranneviss, M. (2013). Surface Modification Methods for Improving the Dyeability of Textile Fabrics. *Eco-Friendly Textile Dyeing and Finishing*. https://doi.org/10.5772/53911

Sreenivasulu, S., & Reddy, A. chennakeshava. (2014). *Mechanical Properties Evalution of Bamboo Fiber Reinforced Composite Materials*. *5013*(3), 187–194.

Sundar, S., Kundu, J., & Kundu, S. C. (2010). Biopolymeric nanoparticles. *Science and Technology of Advanced Materials*, *11*(1), 014104. https://doi.org/10.1088/1468-6996/11/1/014104

Susilowati, S. E., & Sumardiyanto, D. (2018). *Assessing Mechanical Properties of Pineapple Leaf Fibre (PLF) Reinforced Composites for Automotive Applications*. *8*(3), 57–63. https://doi.org/10.5923/j.cmaterials.20180803.02

Tasdemir, M., Kocak, D., Usta, I., & Akalin, M. (2008). *Properties of Recycled Polycarbonate / Waste Silk and Cotton Fiber Polymer Composites*. *November 2014*. https://doi.org/10.1080/00914030802089138

Venkata Reddy, G., Venkata Naidu, S., & Shobha Rani, T. (2008). Impact properties of kapok based unsaturated polyester hybrid composites. *Journal of Reinforced Plastics and Composites*, *27*(16–17), 1789–1804. https://doi.org/10.1177/0731684407087380

Verbič, A., Gorjanc, M., & Simončič, B. (2019). Zinc Oxide for Functional Textile Coatings: Recent Advances. *Coatings*, *9*(9), 550. https://doi.org/10.3390/coatings9090550

Wang, Hai-yan, Chen, Y., & Zhang, Y. (2015). Processing and characterization of powdered silk micro- and nano fi bers by ultrasonication. *Materials Science & Engineering C*, *48*, 444–452. https://doi.org/10.1016/j.msec.2014.12.028

Wang, Hongguang, Xian, G., & Li, H. (2015). Grafting of nano-TiO 2 onto flax fibers and the enhancement of the mechanical properties of the flax fiber and flax fiber / epoxy composite. *COMPOSITES PART A*, *76*, 172–180. https://doi.org/10.1016/j.compositesa.2015.05.027

Wang, J., Guan, J., Hawkins, N., & Vollrath, F. (2018). Analysing the structure and glass transition behaviour of silks for archaeology and conservation. *Journal of the Royal Society Interface*, *15*(139). https://doi.org/10.1098/rsif.2017.0883

Www.planning.go.ke. (2012). *Kenya Vision 2030 REPUBLIC OF KENYA July - August,*

2007.

Xiao, X., Liu, X., Chen, F., Fang, D., Zhang, C., Xia, L., & Xu, W. (2015). Highly Anti-UV Properties of Silk Fiber with Uniform and Conformal nanoscale TiO2 Coatings via Atomic Layer Deposition. *ACS Applied Materials and Interfaces*, *7*(38), 21326–21333. https://doi.org/10.1021/acsami.5b05868

Yang, Y., Zhao, D., Xu, J., Dong, Y., Ma, Y., Qin, X., Fujiwara, K., Suzuki, E., Furukawa, T., Takai, Y., & Hamada, H. (2018). Mechanical and optical properties of silk fabric/glass fiber mat composites: an artistic application of composites. *Textile Research Journal*, *88*(8), 932–945. https://doi.org/10.1177/0040517517690621

Yogesha.B, & Sanjay. (2018). *Studies on hybridization effect of jute / kenaf / E-glass woven fabric epoxy composites for potential applications : Effect of laminate stacking sequences*. https://doi.org/10.1177/1528083717710713

Zhang, H., Zhu, L., & Sun, R. (2014). *Structure and Properties of Cotton Fibers Modified with Titanium Sulfate and Urea under Hydrothermal Conditions*. *9*(1).

APPENDIX: PLAGIARISM AWARENESS CERTIFICATE

SR077

EDU 999 THESIS WRITING COURSE

PLAGIARISM AWARENESS CERTIFICATE

This certificate is awarded to

TUMUSIIME GODIAS

TEC/PGMT/08/18

In recognition for passing the University's plagiarism

Awareness test with a similarity index of 2% and

Striving to maintain academic integrity

Awarded by:

Prof. John Changách, CERM-ESA Project Leader

01st /06/2022